AD-A093 298 NORTHROP CORP ROLLING MEADOWS IL DEFENSE SYSTEMS DIV F/G 9/1
NOISE STUDIES ON INJECTED-BEAM CROSSED-FIELD DEVICES.(U)
NOV 80 G DOHLER, R R MOATS F49620-79-C-0220
UNCLASSIFIED DSD-094-009652 AFOSR-TR-80-1320 NL

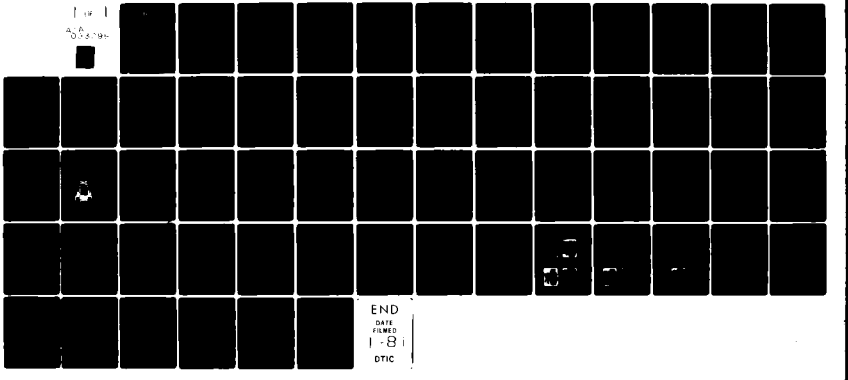

END
DATE FILMED
1-81
DTIC

AFOSR-TR- 80 - 1320

LEVEL II

12

AD A093298

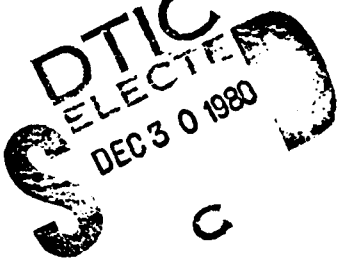

DDC FILE COPY

Approved for public release;
distribution unlimited.

80 12 29 096

(16) 2305 (17) C1

(4) Final technical rept. 1 Jul 79-30 Jun 80,

(UNCLASSIFIED)

SECURITY CLASSIFICATION OF THIS PAGE (When Data Entered)

REPORT DOCUMENTATION PAGE	READ INSTRUCTIONS BEFORE COMPLETING FORM
(9) 1. REPORT NUMBER (18) AFOSR-TR-80-1320	2. GOVT ACCESSION NO. AD-A093298	3. RECIPIENT'S CATALOG NUMBER
(6) 4. TITLE (and Subtitle) Noise Studies on Injected-Beam Crossed-Field Devices.	5. TYPE OF REPORT & PERIOD COVERED Final 07/01/79 - 06/30/80
(14)	6. PERFORMING ORG. REPORT NUMBER DSD-094-009652
(10) 7. AUTHOR(s) G. Dohler, R.R. Moats	(15) 8. CONTRACT OR GRANT NUMBER(s) F49620-79-C-0220 F33615-79-C-1806
9. PERFORMING ORGANIZATION NAME AND ADDRESS Northrop Defense Systems Division 600 Hicks Rd. Rolling Meadows, IL. 60008	10. PROGRAM ELEMENT, PROJECT, TASK AREA & WORK UNIT NUMBERS 2305/C1 61102F
11. CONTROLLING OFFICE NAME AND ADDRESS Air Force Office of Scientific Research Building 410, Bolling AFB, D.C. 20332	(11) 12. REPORT DATE November 1980 13. NUMBER OF PAGES 59
14. MONITORING AGENCY NAME & ADDRESS(if different from Controlling Office) (12) (60)	15. SECURITY CLASS. (of this report) Unclassified 15a. DECLASSIFICATION/DOWNGRADING SCHEDULE

16. DISTRIBUTION STATEMENT (of this Report)
Approved for Public Release - Distribution Unlimited

17. DISTRIBUTION STATEMENT (of the abstract entered in Block 20, if different from Report)

18. SUPPLEMENTARY NOTES

19. KEY WORDS (Continue on reverse side if necessary and identify by block number)
Electron Tubes, Crossed Field Tubes, Electron Guns

20. ABSTRACT (Continue on reverse side if necessary and identify by block number)
The purpose of the work reported here was to investigate experimentally noise and instabilities in crossed-field electron guns, and to correlate noise measurements with beam configuration as measured in the beam analyzer developed by Northrop with Air Force support. The beam tester measures beam location by collisions which take place between the electron beam and a helium molecular beam injected at right angles to the electron beam.

DD FORM 1 JAN 73 1473 EDITION OF 1 NOV 65 IS OBSOLETE (UNCLASSIFIED)

409213

SECURITY CLASSIFICATION OF THIS PAGE (When Data Entered)

NOISE STUDIES ON INJECTED-BEAM CROSSED-FIELD DEVICES

G. Dohler, R. R. Moats

Northrop Corporation

Defense Systems Division

600 Hicks Road

Rolling Meadows, Illinois 60008

November 1980

Final Technical Report for

Period 1 July 1979 - 30 June 1980

Air Force Office of Scientific Research

Building 410

Bolling Air Force Base, D.C. 20332

FORWORD

This report was submitted by Northrop Corporation, Defense Systems Division, to the Air Force Office of Scientific Research, Bolling Air Force Base, D.C.

Lt. Col. Gardner is the project engineer.

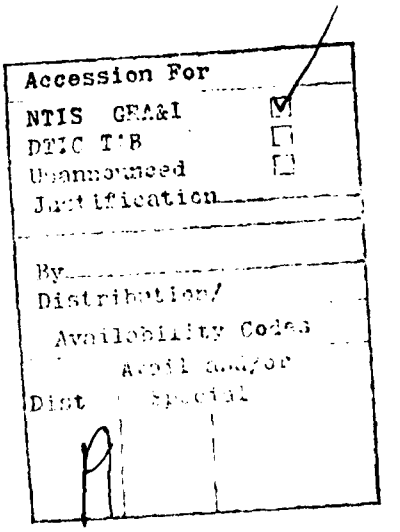

AIR FORCE OFFICE OF SCIENTIFIC RESEARCH (AFSC)
NOTICE OF TRANSMITTAL TO DDC
This technical report has been reviewed and is approved for public release IAW AFR 190-12 (7b).
Distribution is unlimited.
A. D. BLOSE
Technical Information Officer

TABLE OF CONTENTS

SECTION I
INTRODUCTION

The development of stable crossed-field high convergence guns remains a significant technological problem in the continuing improvement of injected beam crossed field devices and to the development of new types of millimeter-wave devices such as the gyrotron. Crossed-field guns are of concern to the Air Force in injected-beam crossed-field amplifiers (IBCFA's) and crossed-field backward-wave oscillators (M-BWO's). Both of these types of devices are presently used in ECM. The IBCFA also represents a possible power source for multi-function radar. In the gyrotron, where magnetron injection guns are used, noise under crossed-field conditions is a limiting factor in the performance of the gun.

The beam characteristics of an X-band IBCFA for multi-function radar, now under development at Northrop*, are of special concern. The performance of the radar in some modes of operation requires low noise output, and in particular low phase noise. The cathode emitter area is severely limited in such an X-band device. Efforts to increase the cathode area by lengthening in the direction of electron travel are expected to increase beam noise, as discussed in Section II.

The work reported here was directed toward the investigation of the most serious problem existing in crossed-field guns, the stability problem, and to relate beam stability to measured beam configuration. The primary experimental tool was the unique crossed-field beam tester recently developed by Northrop with Air Force support [1,2]. This device was designed to

* Contract No. F33615-79-C-1806.

F33615-79-C-2220

measure beam location and relative current distribution in the interaction space of IBCFD's (injected-beam crossed field devices). This category of devices includes both IBCFA's and M-BWO's. This beam analyzer was modified to accomplish the following additional tasks:

(1) Measure the electron beam characteristics in the gun region as well.

(2) Detect noise in the beam.

(3) Interrupt or "chop" the beam to improve reliability of measurements.

In the beam analyzer, a gas beam is injected at a right angle to the electron beam. The atoms in the gas beam are excited by collision with the electrons, and the photons which are emitted are focussed and counted as a function of position. (For more details of the beam analyzer, see Section III.) A level of radiation was observed with the gas beam off which obscured the results. To overcome this problem, a "chopper" for the gas beam was introduced with which, at each location where measurements were made, photon counts were made over equal time periods with the gas beam on and off, and the output of the photon counter is the difference between the two different counts. The results obtained by this method are considered much more reliable than those previously obtained.

The results presented here show the measured beam characteristics both in the gun and the simulated interaction space, and correlation with noise measurements. The electron gun which was the primary subject of this study was a Kino type ungridded gun, for which calculations are easily accomplished. A dramatic decrease in beam noise was found under temperature limited conditions. Such an observation is generally con-

sistent with results observed by many workers. It is supported by some theoretical work and contradicts other theoretical work.

SECTION II
NOISE IN CROSSED-FIELD GUNS

2.1 Noise Generating Mechanisms

In the history of crossed-field guns, the gun configurations most used have been parallel-plate optics and space-charge optics, in which the electrodes are shaped to take space charge into account. The space-charge optics, which are of most interest, were first studied at Thomson-CSF. Further studies were made by Kino and his collaborators, and two analytical design methods were developed, for a "short" Kino gun and a "long" Kino gun. Only the "long" Kino gun is of practical interest for high power cross-field devices.[3]

Experiments by Midford and Kino [4,5] show good agreement with calculations for the short and the long guns in terms of the current-voltage relationships. It was observed, however, that instabilities caused the beam to spread, and "that some unknown strong noise generating mechanism is operating in the cathode region". Much improvement was made by moving the exit plane of the gun closer to the drift region. It is now a well-established design procedure to shorten the transition from gun to interaction space in IBCFA's and MBWO's, and experience shows "the shorter the better".

In spite of the success achieved with guns taking static space charge into account, it was clear that dynamic (i.e., time varying) space charge affected the behavior of the beam. Two factors which seemed to give rise to these effects appeared to be in the noise generated near the cathode surface, especially under space-charge limited conditions, and amplification by the diocotron effect of any noise generated in the gun region.

In numerous publications in the 1950's, it was shown that the beam in a crossed-field device is not stable because of the diocotron effect. The diocotron effect is a gain mechanism which results from rf space charge effects in crossed-field beams. It is well understood theoretically and experimentally for thin laminar beams. However, it does not adequately explain the noise phenomena observed in crossed-field tubes. A noise source or sources many orders of magnitude greater than shot noise, and subsequently amplified by diocotron effect, must be postulated. Some of the phenomena observed include, in addition to the observations of Kino and Midford, the following:

a) Sole Current: Even in absence of rf drive power in an IBCFA, very significant numbers of electrons reach the sole which is at a potential several thousand volts negative with respect to the cathode.

b) Beam Noise: Noise figures of more than 100 dB have been measured.

c) Spurious Oscillations: Spurious oscillations and frequency-sensitive noise orders of magnitude greater than thermal noise are observed. The frequency and amplitude depend on all tube parameters.

All of these phenomena are small if the width (perpendicular to the B Field) of the cathode and the magnetic field are low, or if the current density is low. Arnaud found that, for the parallel-plate Charles gun (Figure 1), enhanced noise occurs if the length of the cathode (in the direction of beam flow) is more than about half a cycloid[6], and that for a long Charles gun

the beam at the input of the interaction space is nearly 100% modulated by noise. It is also observed that the enhanced noise is absent or greatly reduced under temperature limited conditions.

The fact that the noise generating process is poorly understood is emphasized by the diversity of results reported. Gautier and co-workers[7] realized a zero-drive stable IBCFA in L-band with an output power of more than 1 MW, where magnetic field, relative cathode length, and beam current were all necessarily high. Mantena[8] measured a noise figure for a long Kino gun of only 3 dB. Smol[9] has described experiments with very long Kino type guns in which the threshold for noise instability is relatively insensitive to cathode length, and in which noise decreases with greater cathode-anode spacing.

The enhanced noise was the subject of numerous experimental and theoretical studies. A large contribution to the understanding was made by Van Duzer, Whinnery, and co-workers of the University of California.[10] It is generally accepted that the enhanced noise under space-charge limited conditions is due to the existence of "critical electrons" which are just able to pass into the stream below the potential minimum, creating an internal feedback, with combined space charge induced motion, over the width of the cathode. The electric field between the cathode surface and the potential minimum has "negative" polarity, i.e., it tends to repel the electrons emitted. Those electrons which have an emission velocity such that they fail to penetrate the potential minimum will acquire an average drift velocity opposite to the direction of beam injection.

This is in effect a feed-back loop. There is no potential minimum under temperature limited conditions, and this feed-back loop then does not exist. While such a feed-back mechanism provides a reasonable qualitative explanation for the observed phenomena, quantitative analyses are not yet known to be adequate.

On the other hand, there has been theoretical work published more recently by several workers which not only fails to predict enhanced noise under space-charge limited conditions, but in fact indicates the contrary: space-charge smoothing: Such results are reported by Harker and Crawford[11], by Shkarofsky,[12] and by Shaw and Kooyers,[13] all working under AFOSR support. The first two of these represent purely theoretical analyses, and the last represents the results obtained from a computer model.

2.2 Gun Designs with Improved Stability

If the instability of the beam is due to a feed-back of the electrons in the potential minimum region, it should be possible to stabilize the beam by interrupting the feed-back loop. Two methods have been studied, inhomogeneous magnetic field, and the gridded gun.

If there is small component of magnetic field perpendicular to the cathode, the pattern of electron motion in the potential minimum region is perturbed, and the critical electrons do not move back to the point of origin. A number of workers have reported an appreciable reduction of noise, or of noise/signal ratio, with such a perpendicular B field [14,15,16]

Arnaud and Doehler[17] studied a gridded gun with the aim of interrupting the feed-back loop in the potential minimum. The grid wires were in the direction of the magnetic field. A significant reduction of the noise and the sole current was observed. Figure 2 shows the ratio of the noise current measured around 50 MHz in a bandwidth of 4 kHz, as a function of B/B_{cr}. B_{cr} is the critical magnetic field for cut-off corresponding to the anode voltage which is applied, and B is the actual magnetic field. Curve 1 corresponds to the normal Charles gun. The enhanced noise starts at $B/B_{cr} \simeq .6$. Curves 2 and 3 were measured with a grid-to-cathode spacing of 10 mm.

Diamand[18] obtained a reduction of the noise figure in an L-band 200-watt IBCFA from about 100 dB to 50 dB, using a high-μ grid with wires perpendicular to the magnetic field. Figure 3 shows the measured noise figure versus plate voltage at constant current. The grid voltage was varied to maintain constant current. In this case, the noise decreased with higher cathode temperature limited conditions.

Grids have been found essential for most practical IBCFA applications for beam current switching at low voltage, and are therefore an almost universal requirement in modern IBCFA's.

SECTION III
TEST APPARATUS

3.1 The Beam Tester

The primary tool for evaluating crossed-field beams is the crossed-field beam tester developed by Northrop under AFAL Contract No. F33615-75-C-1033[1], and refined as an effective instrument for crossed-field gun evaluation under AFAL Contract F33615-78-C-1435[2]. The essential feature of this device is that a gas beam is injected which is perpendicular to the electron beam, gas stoms are excited by collision with electrons and promptly re-radiate the energy from excitation so that the location of the radiation represents essentially the position of the collision. A portion of the photons so generated is focussed on a detector. A schematic of the apparatus is shown in Figure 1. The location of the portion of the beam being probed is determined in the x-y plane by the relative position of the gas jet, and in the z-direction by the location of the slit in front of the detector. More details as to the construction and principles of operation of the beam tester are given in Reference 2.

3.2 Gas Beam Chopper

It has been observed that when the gas beam is shut off, enough photon counts appear to affect the accuracy of beam measurements to a serious degree. Such results were reported in Reference 2, and are shown here in Figures 2 and 3. Possible sources of spurious radiation include the hot cathode, electrons striking electrodes, and electrons colliding with molecules of background gas.

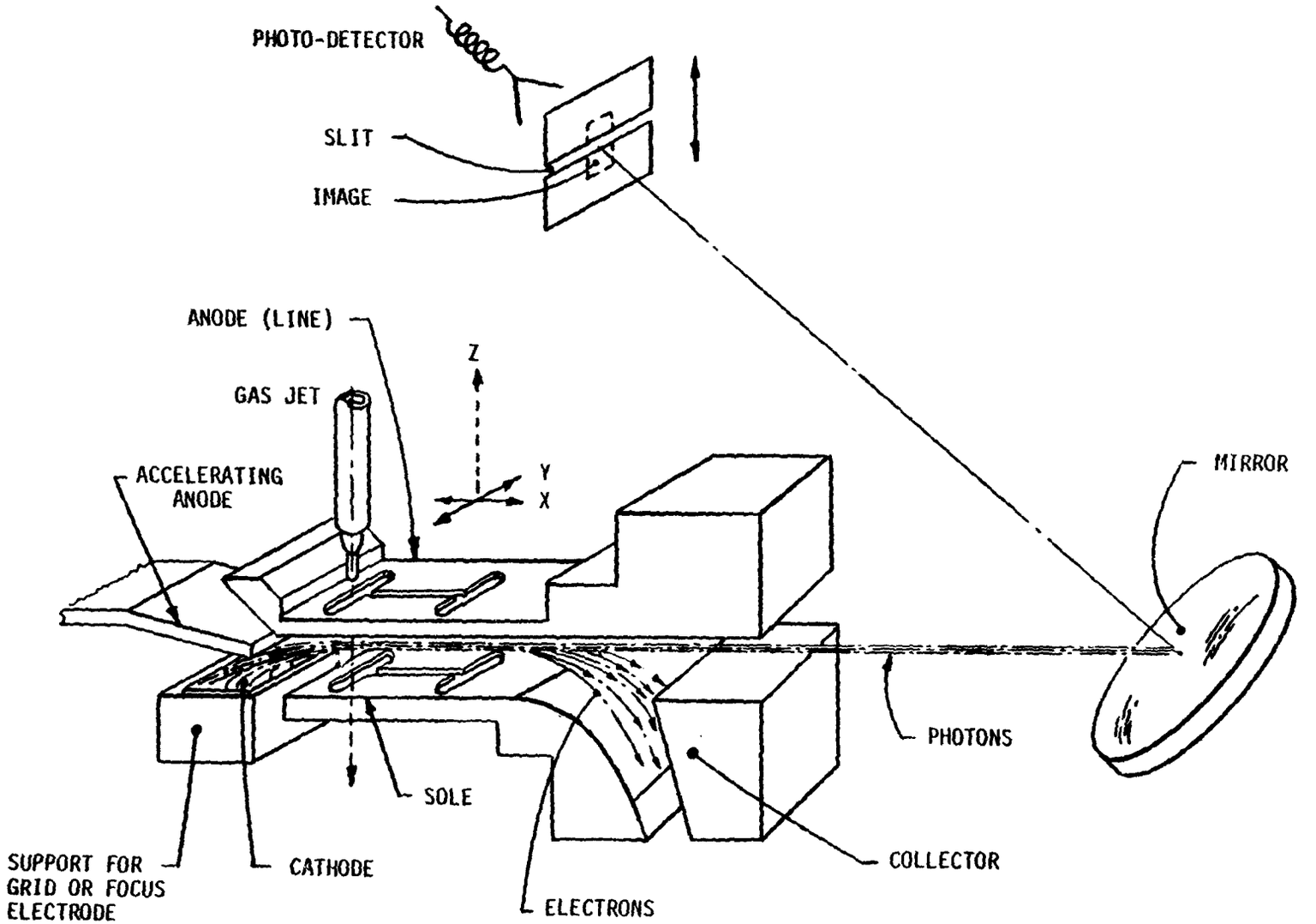

Figure 1. Schematic of Crossed-Field Beam Tester

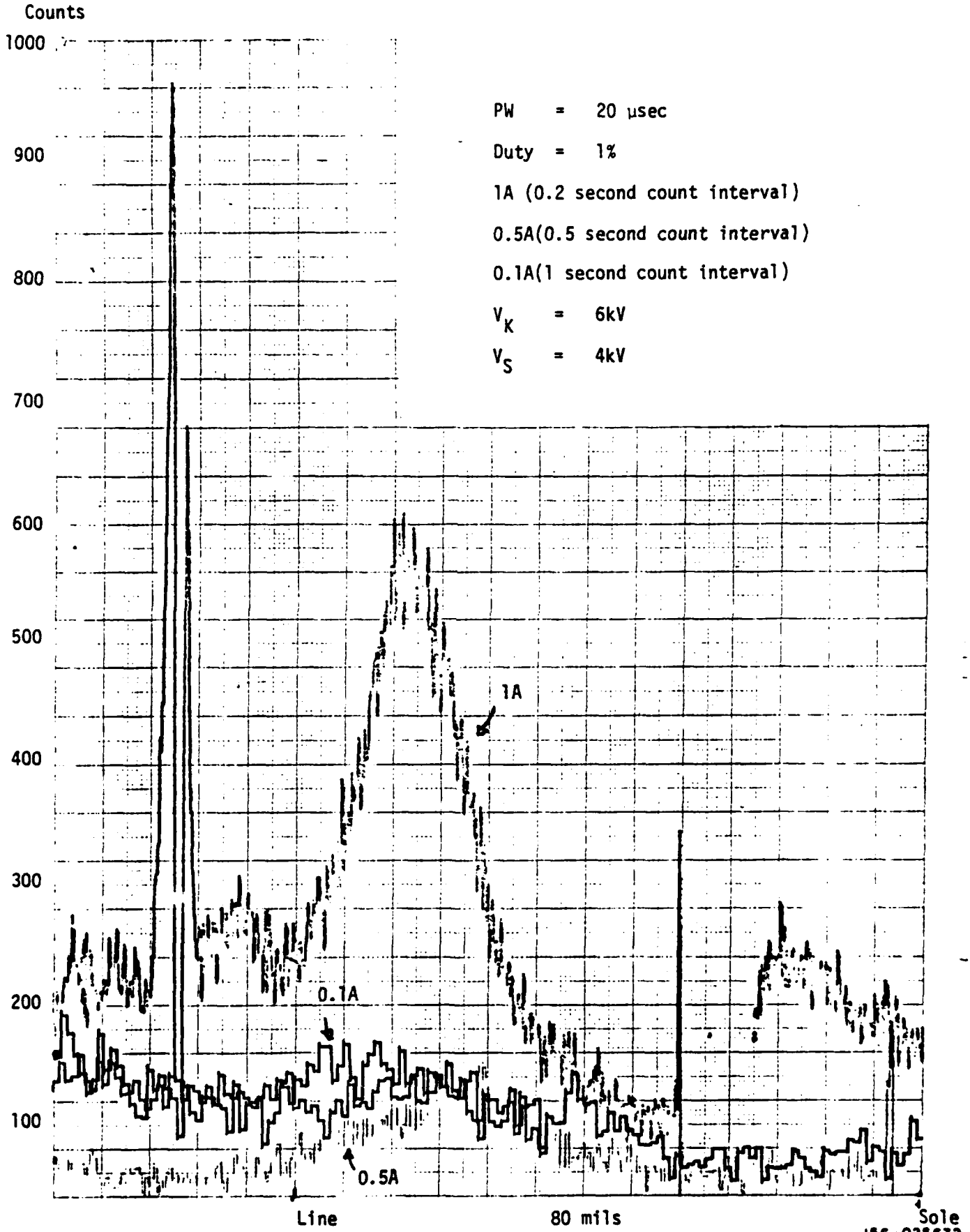

Figure 2. Run A with No Gas Injection

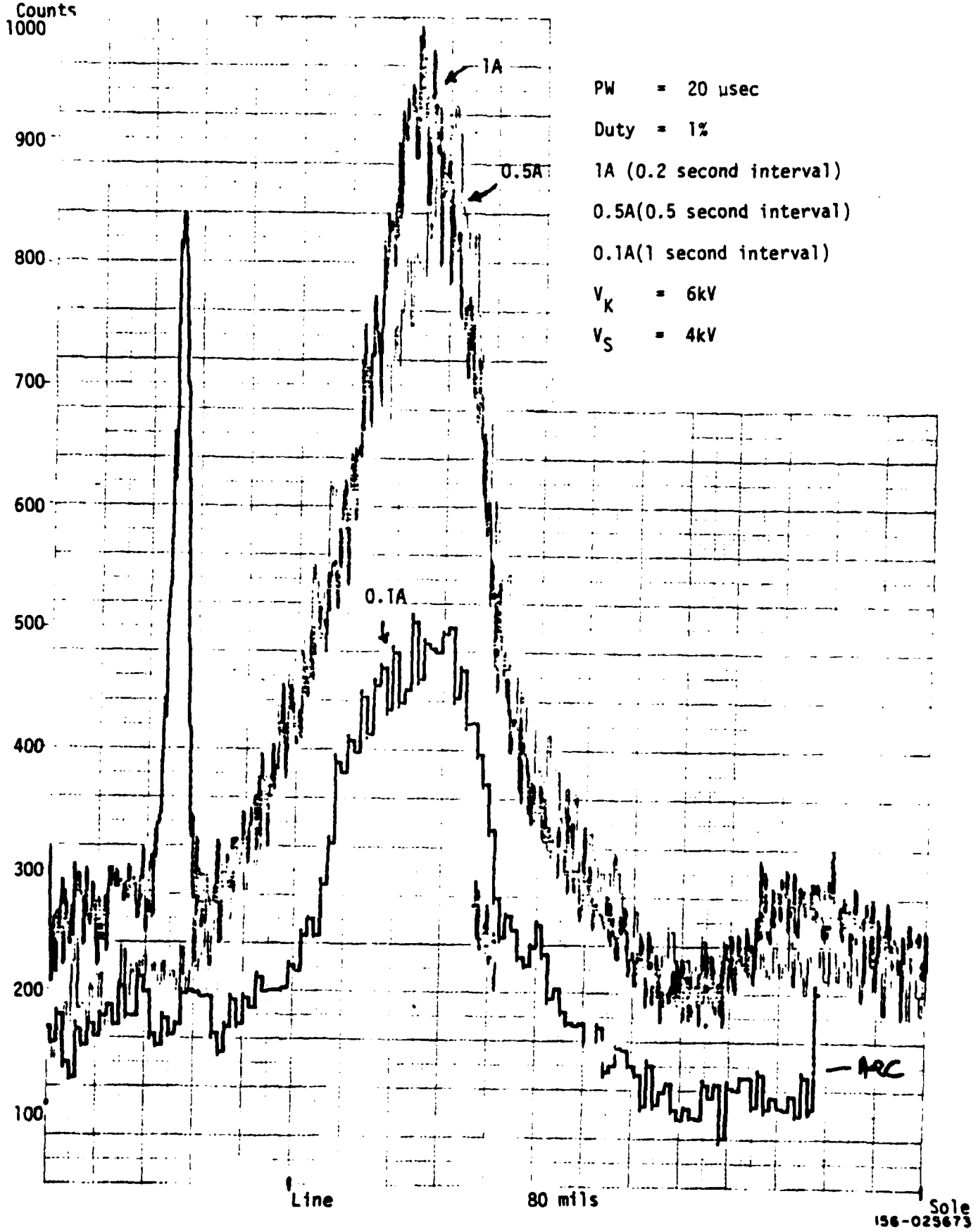

Figure 3. Run A with Gas Injection

An approach to the suppression of these unwanted photon counts is to count photons with the gas beam present and also with the gas beam off for an equal time period, and then to subtract the latter from the former. To accomplish this a vane, or chopper, is provided to interrupt the gas beam when actuated by a solenoid, as shown in Figure 4. At each position of the gas jet and slit, two readings, each over a period which is of the order of magnitude of a second, are made. The counter instrument is programmed to subtract the difference in counts with and without the gas beam, and to output the difference.

3.3 Computer Control and Automation

During the course of this program, the taking of data in the beam analyzer was made fully automated. Each entire experiment, for any one setting of the power supply system, is under the control of an HP-9845A computer. The computer controls the stepping motors which move the gun and magnet assembly in the X-direction and Y-direction, and the slit in the Z-direction. It also controls the solenoid which actuates the "chopper". It collects the data from the counting instrument and automatically plots the results. Examples of the output from automated experiments are shown in Section IV of this report.

3.4 Noise Detector

Noise in the beam is picked up by a short section of a meander circuit, as shown in Figure 5. The meander circuit in combination with the electron beam constitutes, in effect, a crossed-field amplifier without an rf input signal, but the circuit is too short for any real

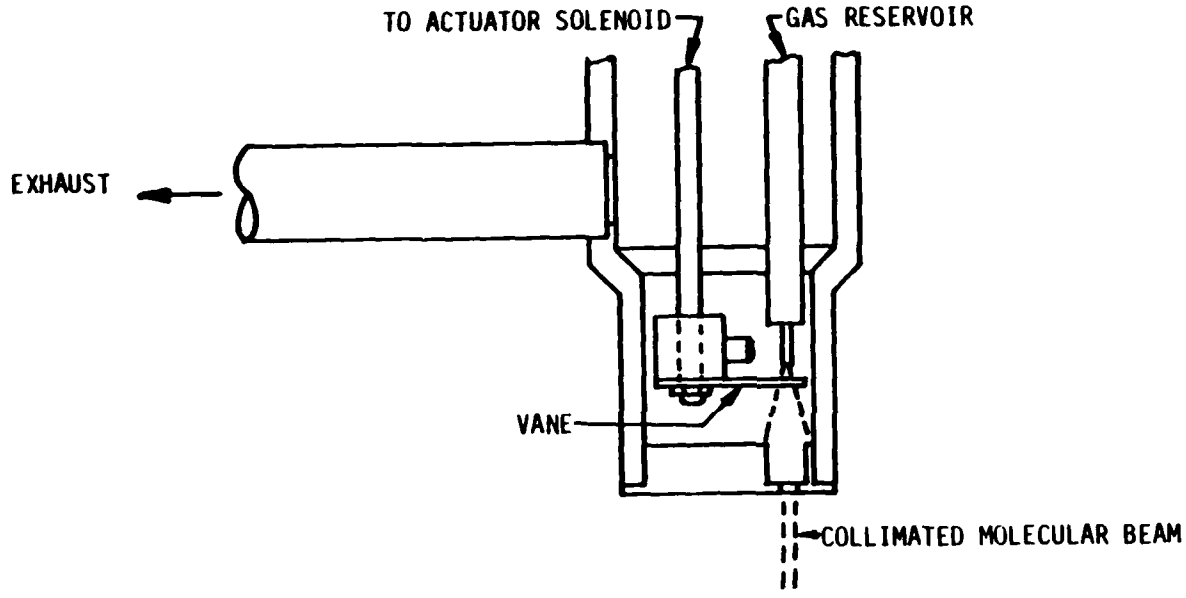

Figure 4. Gas Beam Chopper Mechanism.

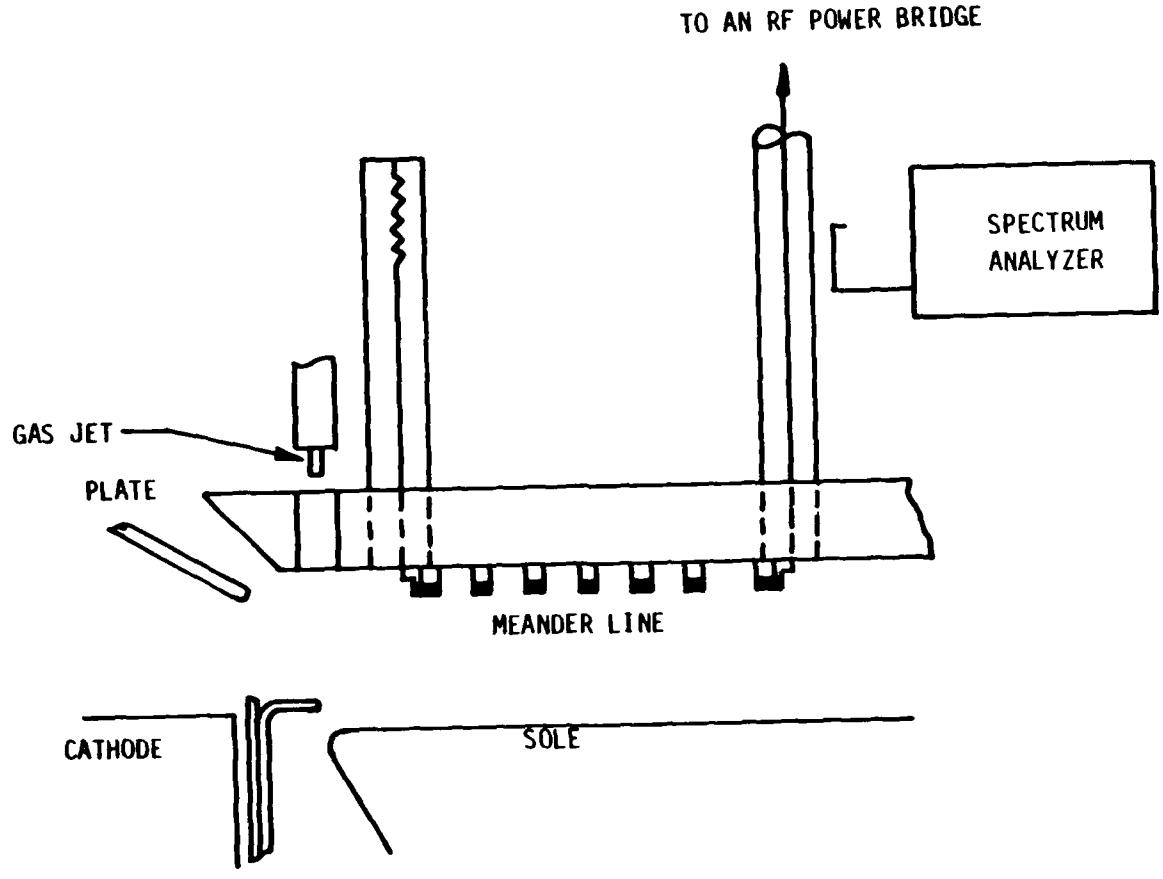

Figure 5. Meander Line Coupling for Measuring Beam Noise.

amplification to take place. The "input" port is replaced by a termination which consists of resistive material on the ceramic supports between the meander and the ground plane. The effective length of the meander circuit, not including the bars which constitute the termination, is 10 circuit bars, or 0.270".

The essential electrical properties of the meander circuit, the delay ratio (c/v_{ph}) and coupling impedance at the level of the circuit, are shown in Figure 6. Over the 10 bars constituting the active portion of the circuit the attenuation is considered negligible. A circuit of this length is too short for accurate measurement of its properties. Therefore calculated values are used. These values are calculated according to a method developed at Northrop under Air Force Contract No. F33615-79-C-1752, which has given excellent correlation with experiment.

The power coupled into the circuit by an ac component of current in the electron beam has been calculated according to well-known small-signal theory for an IBCFA. The work of Gould [19] was used for the basis of calculations. The difference between the IBCFA calculations and the problem of interest here is in the entrance boundary conditions. In the IBCFA, the beam enters the system unmodulated, and there is an rf input signal. In the present case, there is no rf input signal, but there is beam modulation. For a given ac component of current density it is possible to calculate the power level at the output of the meander. The relationship may be expressed as a resistance, R, such that $P = I_1^2 R/2$, where P is the output power and I_1 is the peak value of the AC component of current. In Figure 7 the calculated value of R is shown for two different

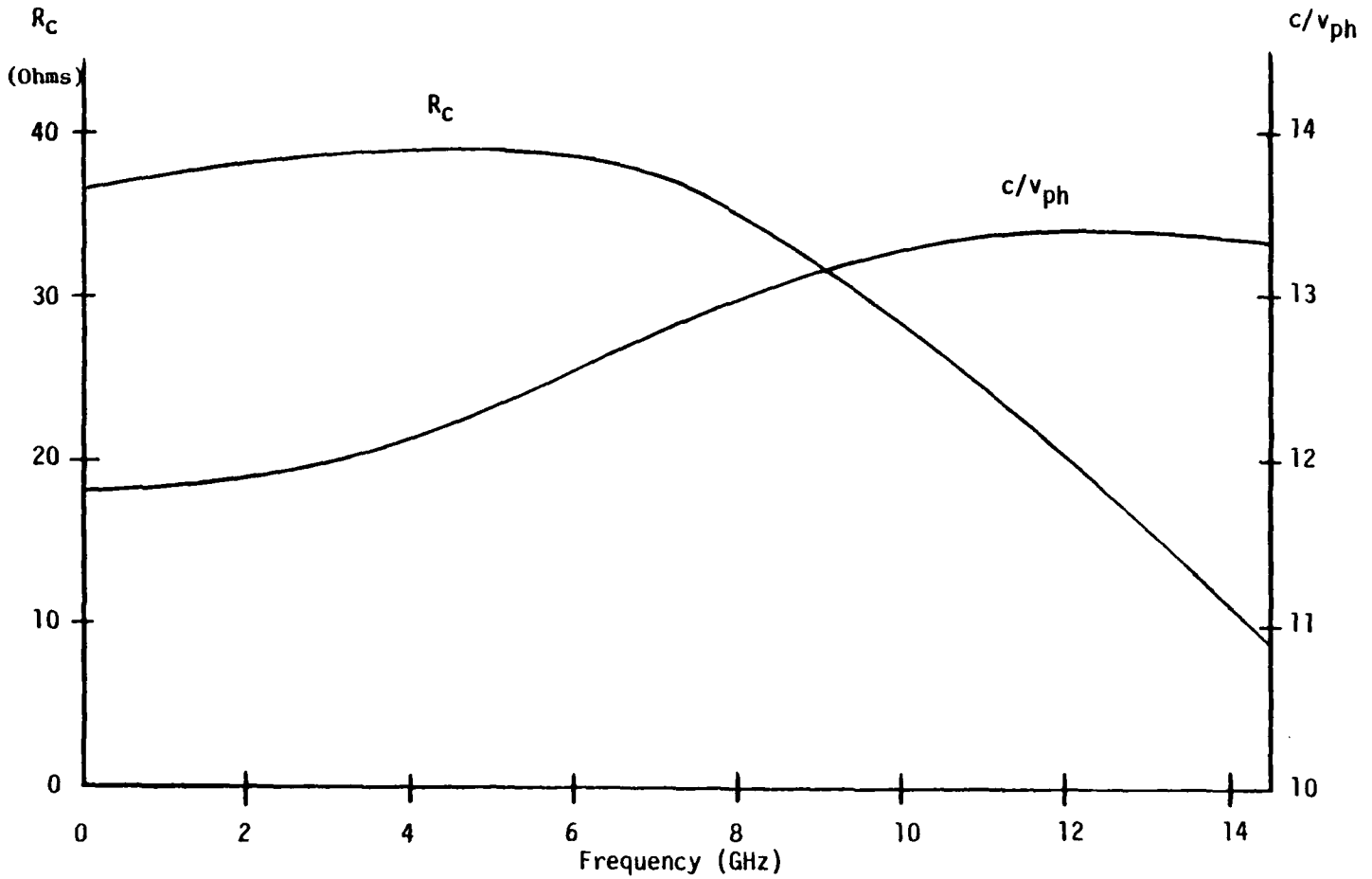

Figure 6. Coupling Impedance (R_C) and Delay Ratio (c/v_{ph}) of Meander Circuit.

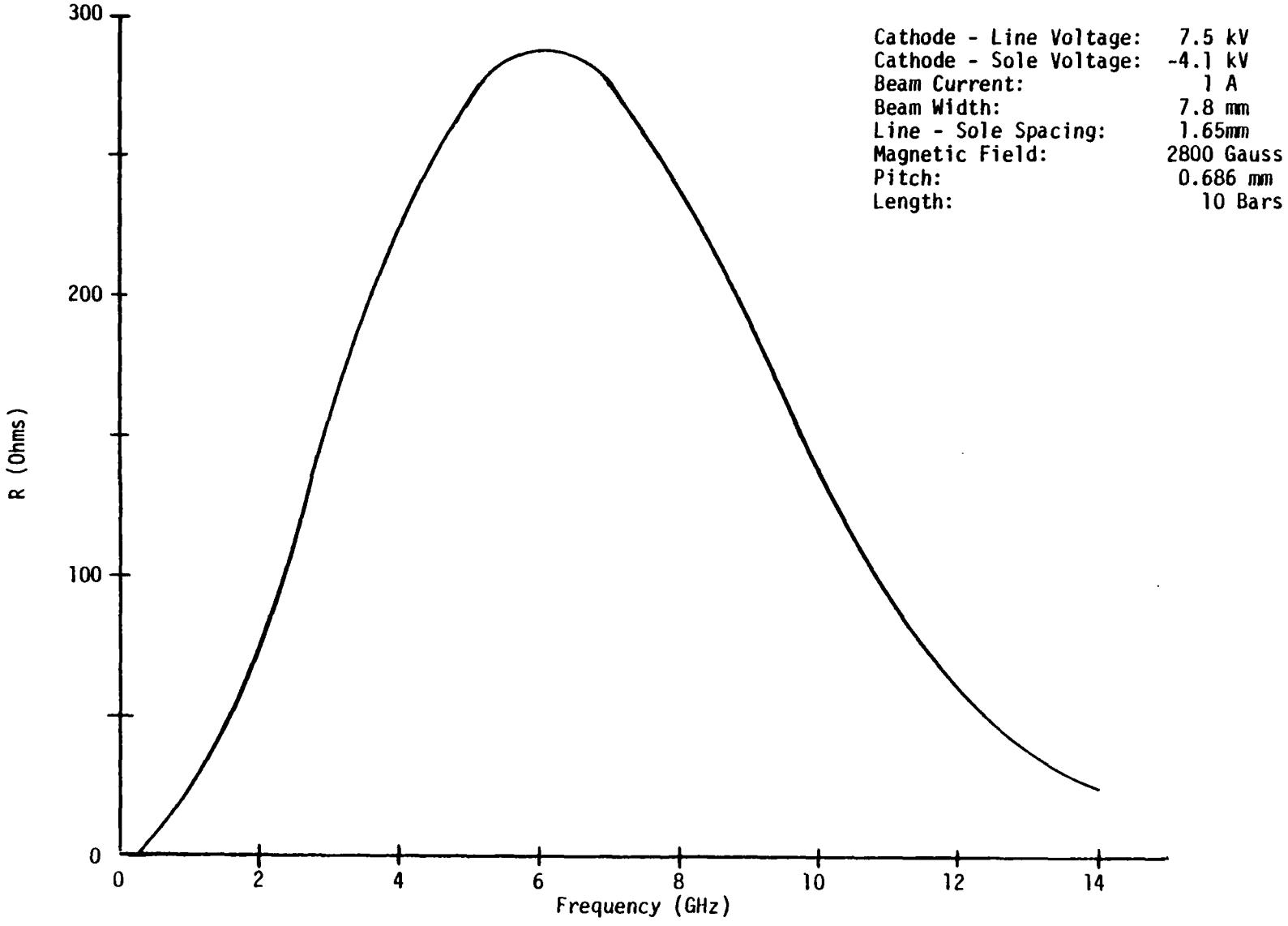

Figure 7. Effective Resistance for Coupling to Beam: Varation with Frequency

values of beam current, and with other parameters the same. This method of analysis also shows that R is not very sensitive to asynchronism between beam velocity and phase velocity of the circuit. In Figure 8 is shown the value of R as a function of the asynchromism parameter, b, as defined by Gould[19] and other authors.

3.5 Electron Guns

The characteristics of electron guns have been studied. The first of these guns is a gridded gun designed for the X-band radar IBCFA previously mentioned. The gridded gun is shown in Figure 9. The grid dimensions were as follows:

Pitch (Center-to-Center of Grid Bars)	0.0182"
Number of Bars	17
Effective Width of Grid Opening	0.324 "
Bar Thickness	0.037 "
Bar Width	0.033 "

Other principal gun dimensions are shown in the figure.

The second gun which was built was a"Kino" type ungridded gun, which was studied for the beam noise generated as well as the beam location. This gun is shown in Figure 10.

In both guns, a slot was placed in the plate electrode (accelerating anode) to allow the gas jet to be introduced into the gun region as well as into the simulated interaction space. The slot in the plate is shown in Figure 11. In the particular configuration used here, note that there is only one transverse slot in the interaction space instead of the two shown in Figure 1.

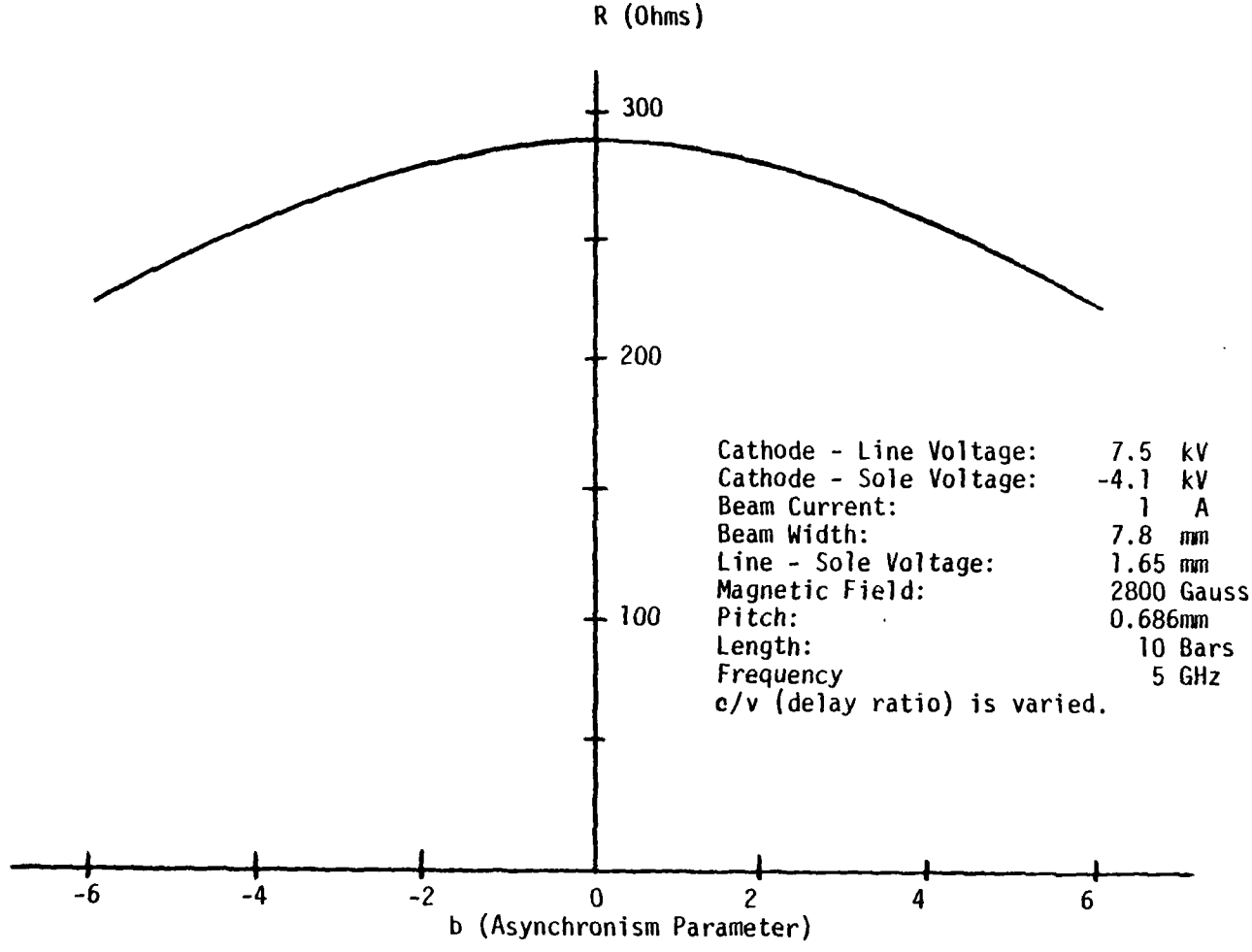

Figure 8. Effective Resistance for *Coupling to Beam: Effect of Asynchronism.*

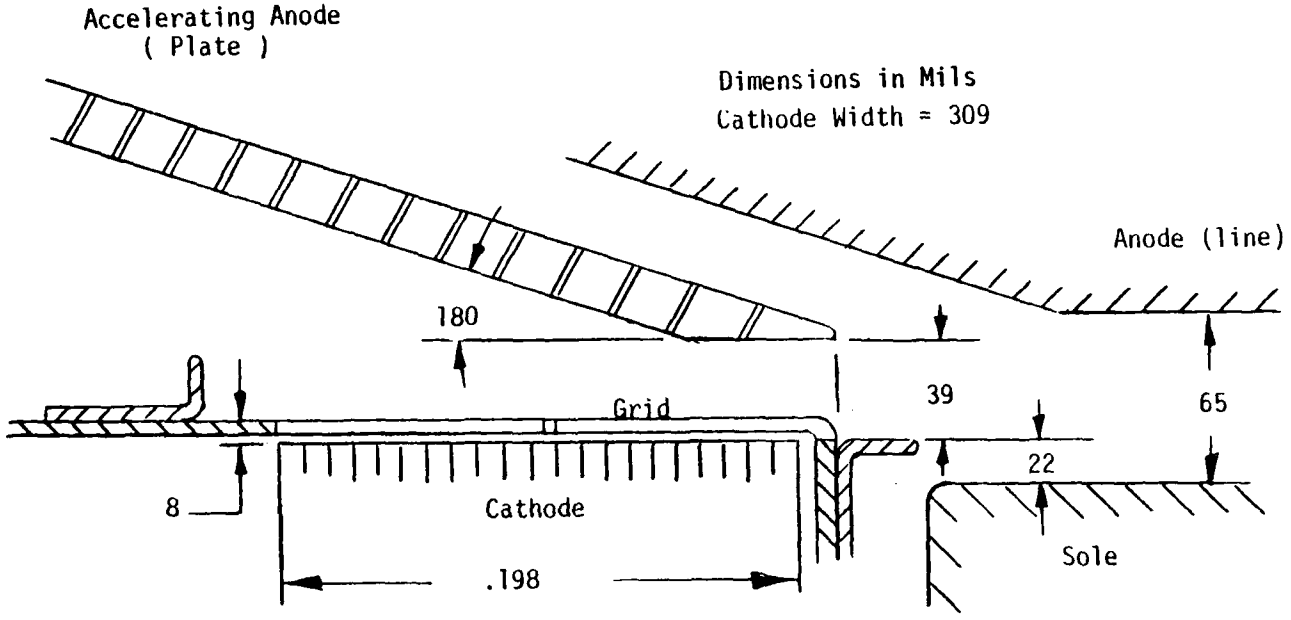

Figure 9. Cross Section of Gridded Gun.

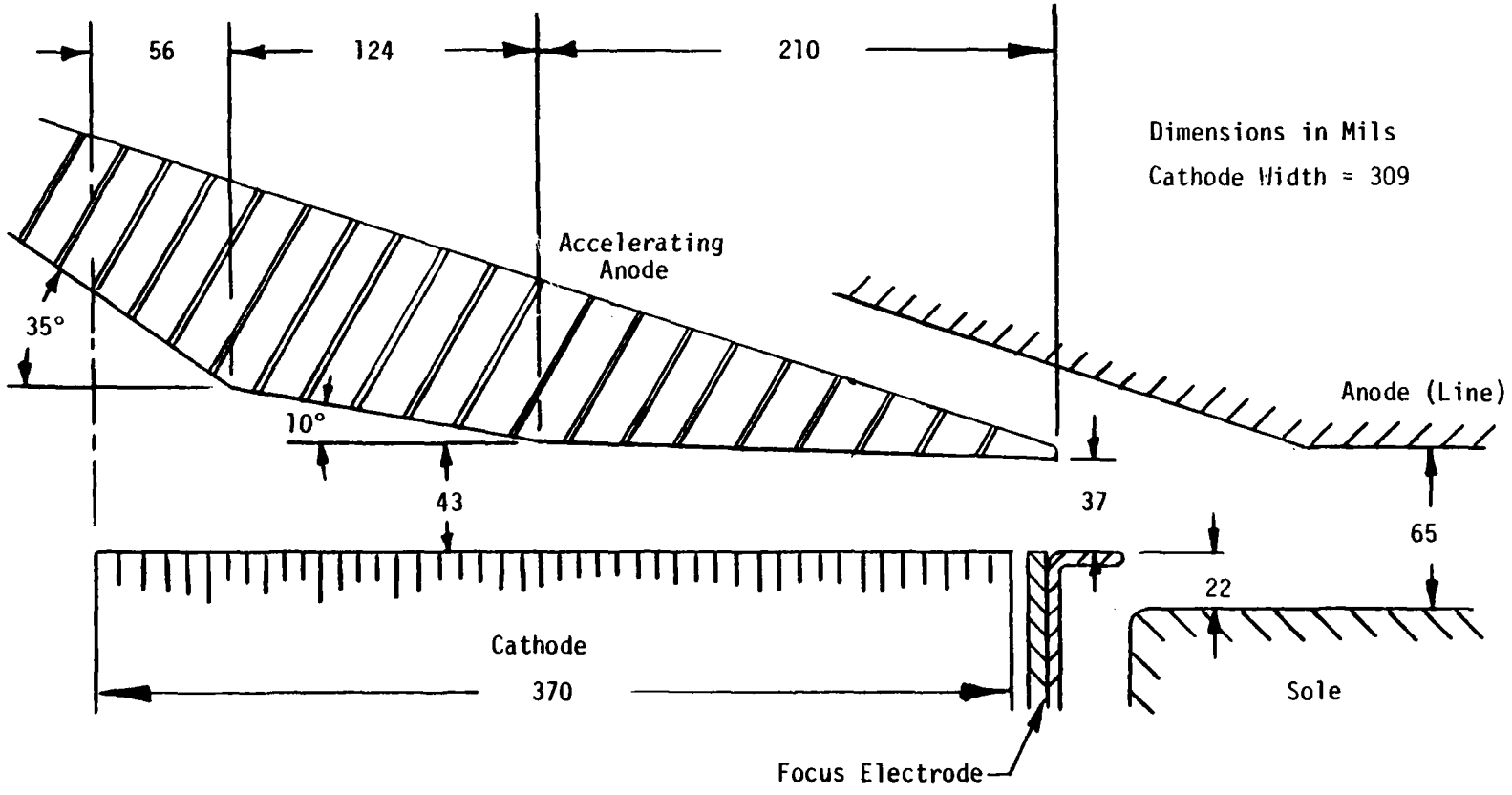

Figure 10. Cross Section of Kino (Ungridded) Gun.

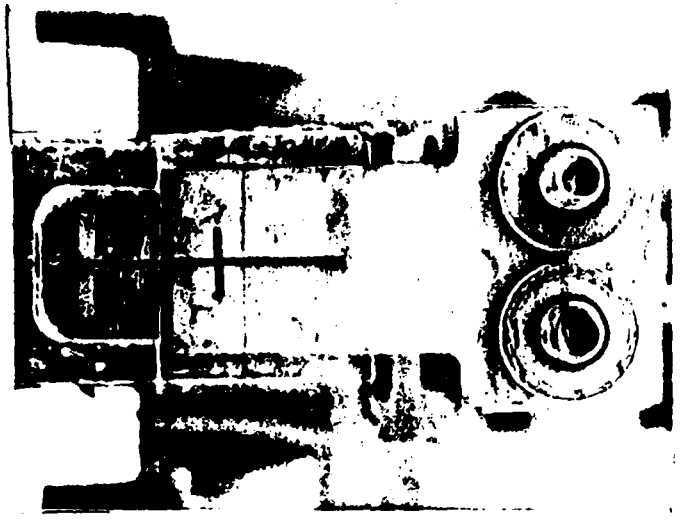

Figure 11. Photograph of Gun and Anode (Line) Assembly, Showing Slots for Injecting Gas Beam.

SECTION IV

MEASUREMENTS

4.1 PRELIMINARY MEASUREMENTS

Measurements of the properties of the gas beam were made to determine the beam spread and hence the resolution in the x-y direction (reference figure 1). This was accomplished by moving the jet across the slot in the center of the beam between the transverse slots. (In normal operation, the jet is always centered over a slot.) Thus, the gas beam is shadowed from the electron beam except when the jet is immediately over the slot. If the gas beam is much narrower than the slot width, as expected, there will be few or no counts produced by collisions with the electron beam when the gas jet is not over the slot. As it moves across the edge of the slot, the counting rate will rise abruptly, and will remain nearly constant while the gas beam moves across the slot. After the gas beam reaches the other edge of the slot, the counting rate will fall abruptly. A set of measured results is shown in figure 12*. The slot width is 0.010 inches, so that the beam is evidently much wider than the slot. Several runs were made with different sets of electron beam parameters, and all of them showed a gas beam width of 0.040 inches to 0.050 inches. Calculations of beam spread were made using the method described in Reference 2, page 10. The following gas beam parameters were used:

---

* In the data presented in this section, the following symbols are used: V_k = cathode-to-ground voltage, where the electrode simulating the circuit (line) is always at ground; V_s = sole voltage with respect to cathode; V_a = accelerating anode voltage with respect to cathode; V_g = grid or focus electrode voltage with respect to cathode; I_k = cathode (beam) current, B = magnetic field (y-direction).

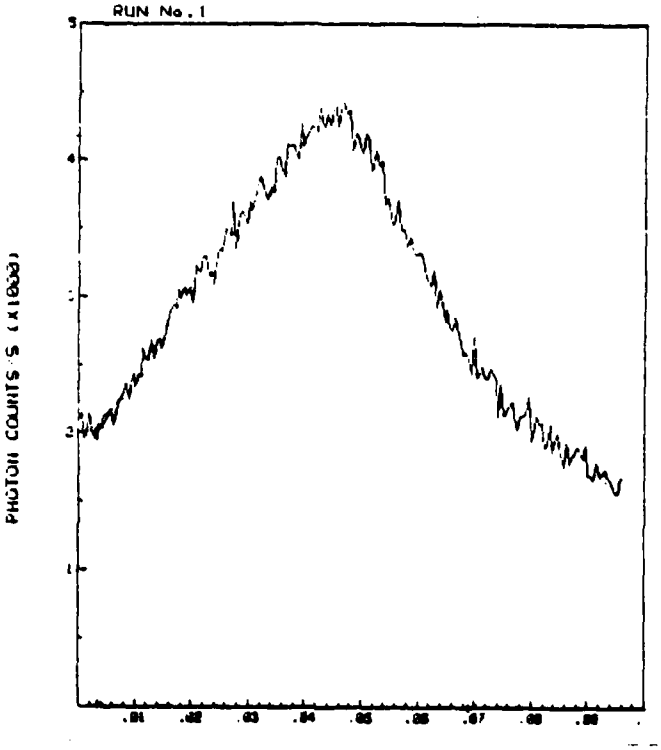

V_k = 4 kV
V_s = -6 kV
V_a = 2.1 kV
V_g = 0 V
I_k = 100 mA
B = 3450Gauss

Figure 12. Gas Jet Beam Spread.

Length of capillary:	1.0 cm
Radius of capillary:	0.0023 cm
Pressure of gas in reservoir:	0.09 Torr
Temperature:	$300^{o}K$
Diameter of He aton:	2.65×10^{-8} cm

The resulting value of the half angle is 0.015 radians. Since the jet was about 0.175 inches above the slot, the observed half angle is 0.025/0.175, or about 0.14 radians. The difference has not yet been explained. However, it is necessary to conclude that the resolution in the x-y plane is no better than $\pm$0.020 inches in the direction of a slot, while the gas beam will be truncated to approximately the width of the slot in the other direction.

The effectiveness of the gas beam "chopper" is illustrated in figure 13. Figure 13(b) shows counts without the chopper, and figure 13(a) shows the results with those counts which appear in absence of the gas beam suppressed. These measurements show photon counts as a function of z-position.

4.2 GRIDDED GUN

The gridded gun shown in figure 9 was mounted in the beam tester after automated measurements were introduced, but without the "chopper" or meander circuit to measure noise. A number of sets of measurements were made, and the results summarized here. In all of the plots of photon counts in this report with the exception of figure 12, photon counts are shown as a function of z-position for a given gas jet location. With respect to the gridded gun data, the anode which simulates the delay line is located at position 0.004 inches on the horizontal axis, and the sole is at position 0.069 inches. The plane of the cathode corresponds to 0.047 inches.

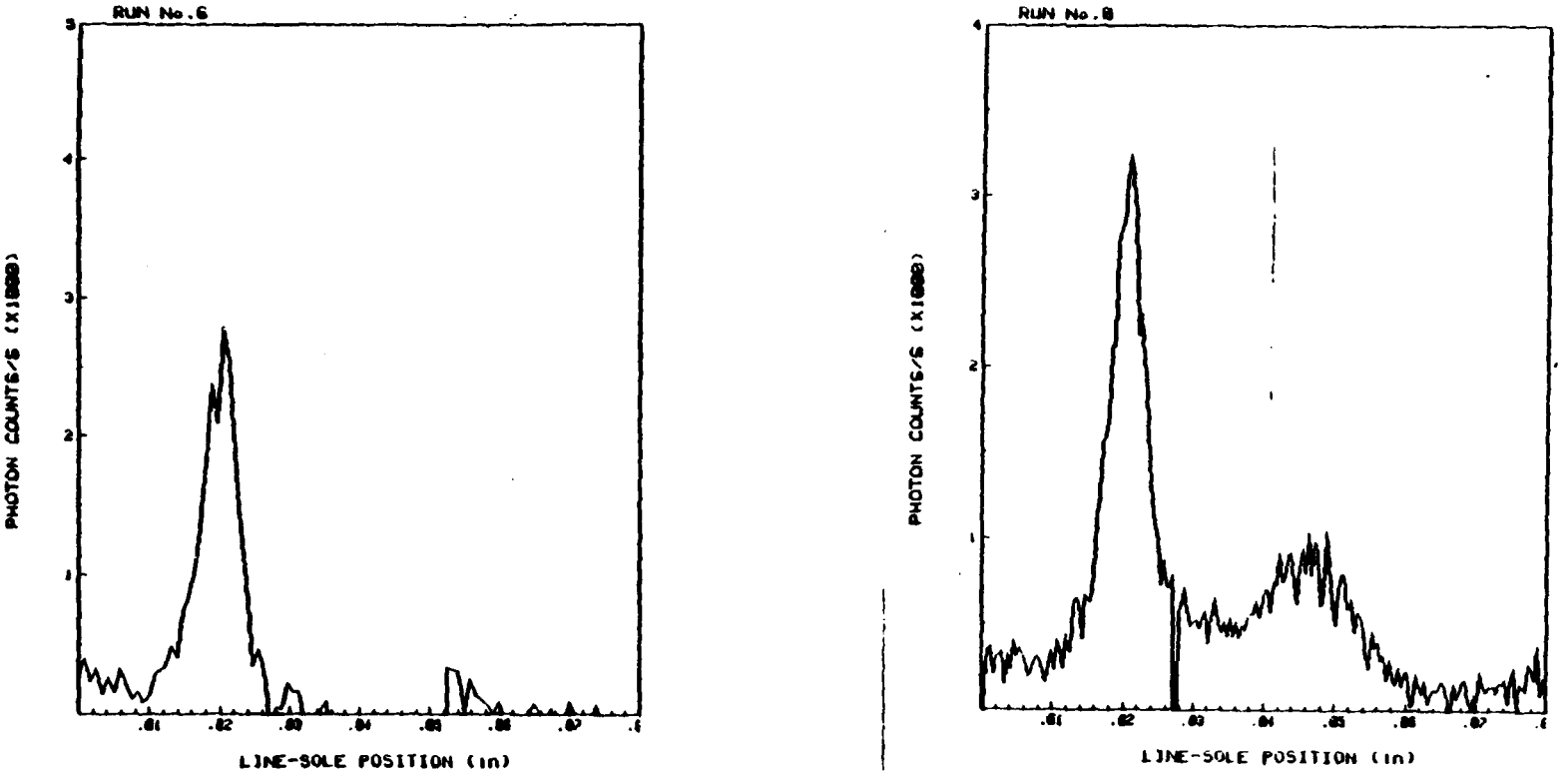

V_k = 3 kV V_g = -400 V
V_s = -6 kV I_k = 100 mA
V_a = 1 kV B = 3450 Gauss

Figure 13. Effect of Gas Jet "Chopper".

A series of measurements was made to determine beam distribution in the transverse direction - the y-direction of figure 1. Each set of data shows photon counts as a function of the accelerating anode and across the slot in the electrode which simulates the delay line of an operating tube. Three of the measurements made in the line anode slot are shown in figure 14, along with a plot of the peak value observed for each set of measurements along the transverse slot in the plate as well as the line anode slot. The beam is mainly concentrated over a width well under 0.180 inches as compared with the cathode width of 0.309 inches. There are two factors which are probable contributors to the beam narrowing: (1) Magnetic field is greater nearer the pole pieces than in the center, and (2) the shields on the edges of the gun and of the sole, which prevent the lateral escape of electrons, tend to push the beam toward the center by electrostatic forces. The location of peak counts in the center of the beam is 0.022 inches from the sole, which corresponds with the calculated ideal beam position within 0.001 inches.

A series of measurements was made to probe the beam position in the gun as a function of grid voltage. As the grid was made more negative, the voltage on the accelerating anode was increased to maintain constant beam current. Two of the plots from this set of measurements are shown in figure 15. The gas jet is 0.050 inches from the back of the cathode on the y-axis center line. When the grid is at -10V with respect to cathode, the peak of counts is 0.0025 inches above the cathode, and when the grid is at -200V, the peak of counts is 0.0065 inches above the cathode. Note that the top side of the grid is 0.008 inches above the cathode. In both plots there is a lesser peak of counts located to the left. These are attributed to gas collisions with the beam in the simulated interaction space. Although no gas is injected in this region, gas will drift from the gun region because there is no escape for it through the cathode surface, whereas means of escape of the gas

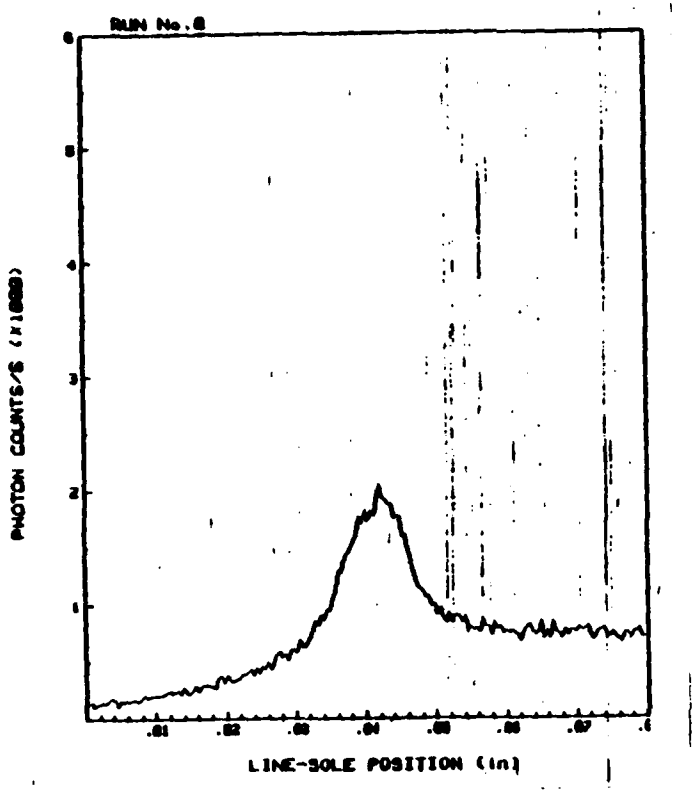

(a) Lateral Position - 0.090"
(Anode Slot)

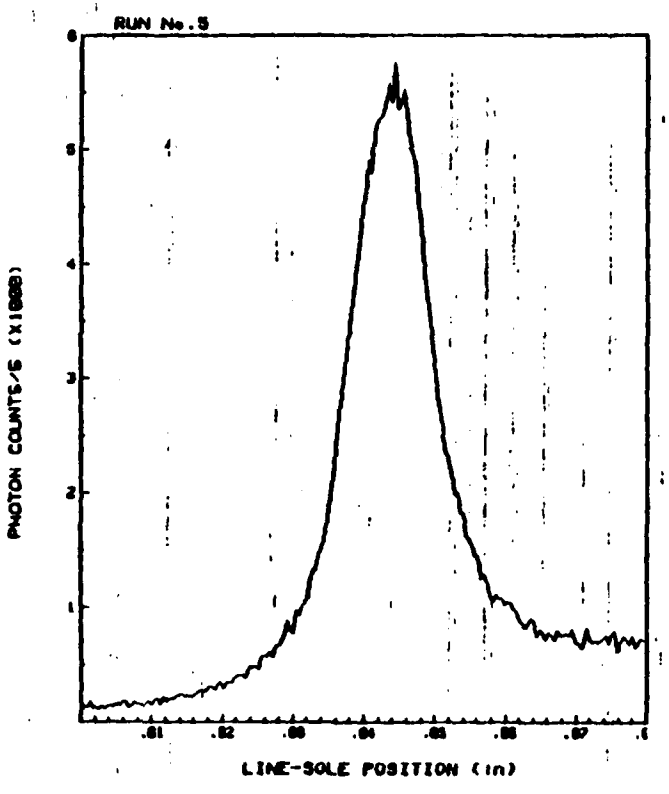

(b) Center (Anode Slot)

V_k = 9.25 kV
V_s = -2.75 kV
V_a = 2.1 kV

V_g = 0
I_k = 100 mA
B^k = 3450 Gauss

Figure 14. Lateral Variation of Beam Density (Continued on Next Page)

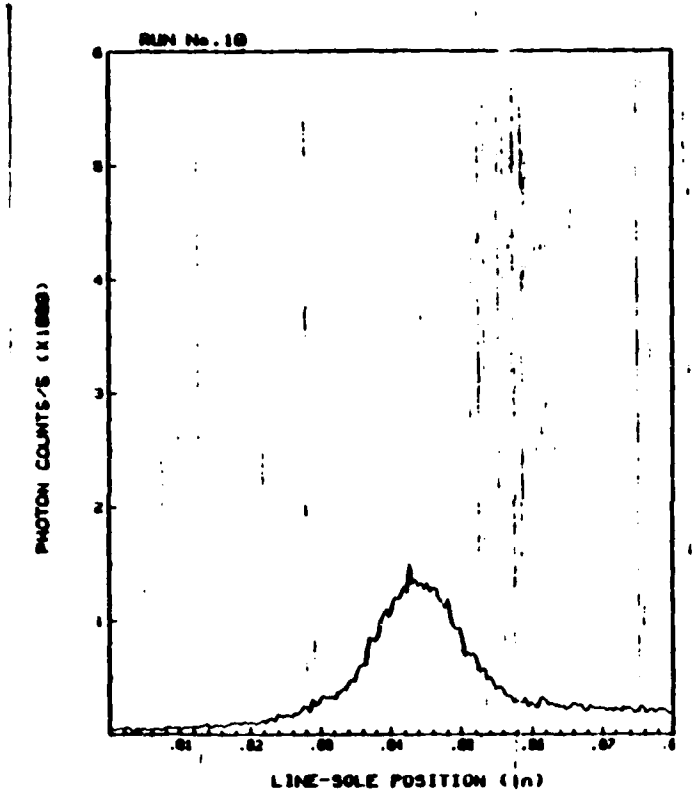

(c) Lateral Position +0.090"
(Anode Slot)

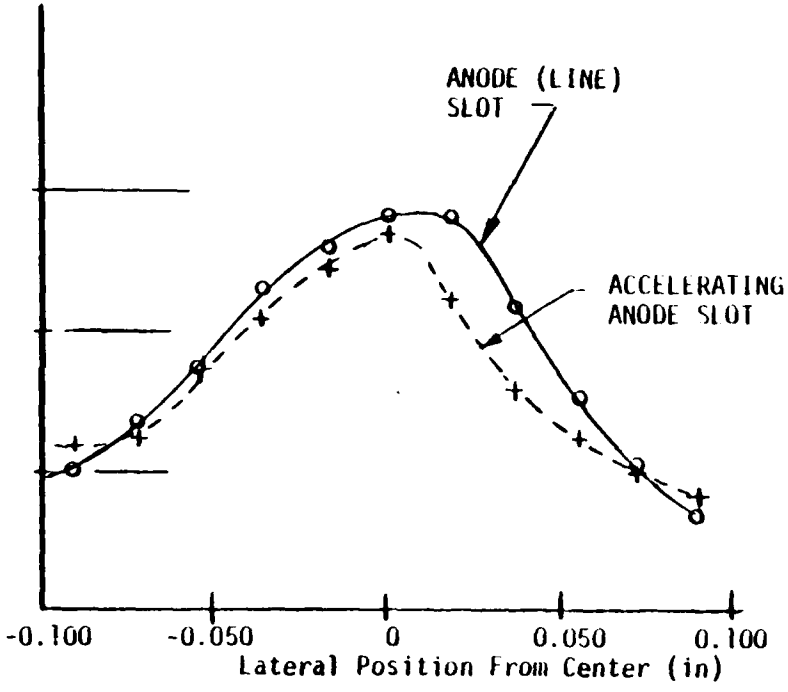

(d) Peak of Counts as Function of Position

Figure 14. Lateral Variation of Beam Density (Continued from Preceding Page).

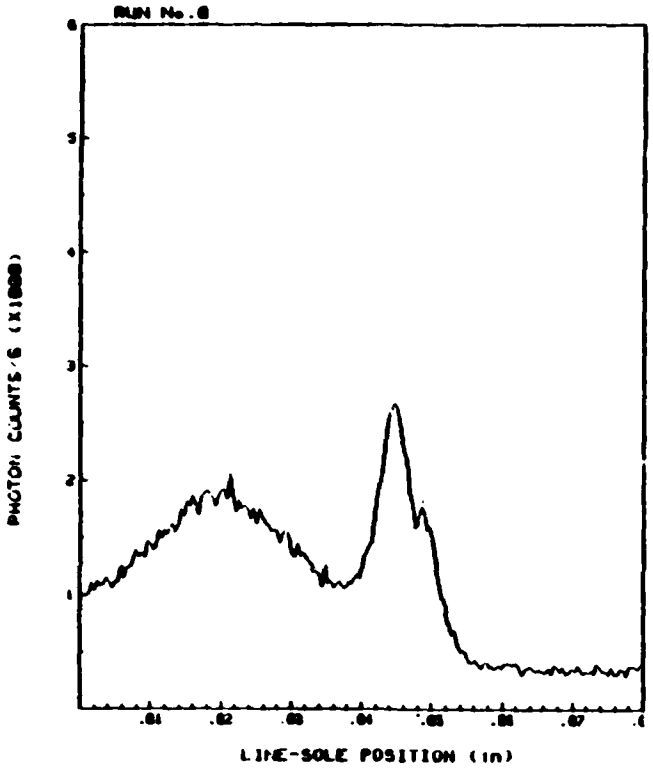

(a) V_a = 1.94 kV, V_g = -10 V

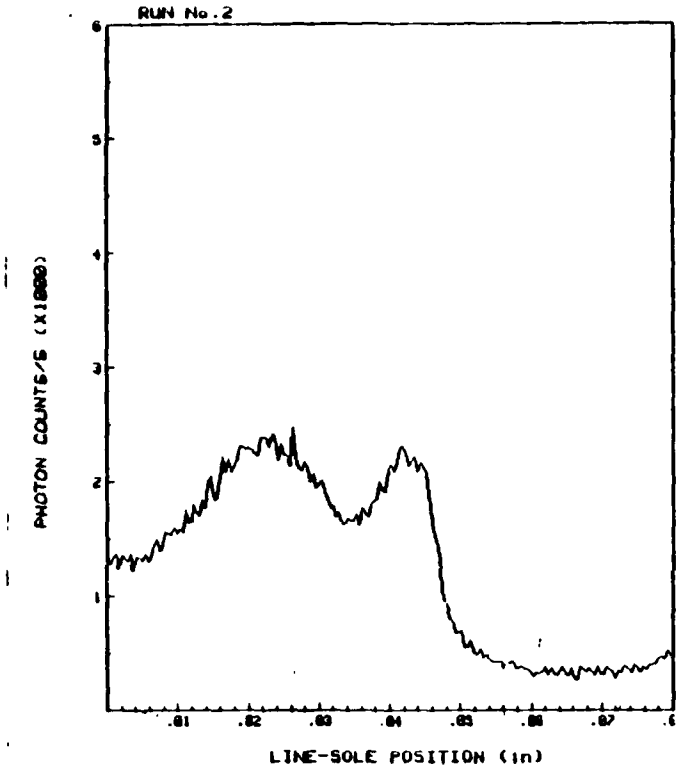

(b) V_a = 3.2 kV, V_g = -200 V

For Both Sets of Data:

V_k = 4.5 kV I_k = 100 mA
V_s = -6 kV B = 3450Gauss

Figure 15. Effect of Grid Voltage on Beam Position for Constant Beam Current.

through the sole surface is provided in the simulated interaction space. These spurious photons shown in figure 15 are poorly focused, but they are counted. This is a limiting factor in probing the beam in the gun region.

An important useful function of the beam tester is to determine the optimum location of the plane of the cathode with respct to that of the sole. The objective is to minimize the beam thickness. A series of measurements is made with constant line-to-sole voltage for constant beam velocity, and with the cathode-to-line voltage varied. A series of 10 such measurements was made using the gridded gun, and four representative sets of data are shown in figure 16. The narrowest peak of counts is in figure 16(b), corresponding to 8 kV from cathode to line, but the peaks in (a) and (c) are not much wider. The beam spread in (d) is much greater and is asymmetrical, skewed toward the anode side at the bottom. This observation is consistent with considerable cycloiding of the trajectories. The observations may be summarized as follows:

Figure	V_k (kV)	V_s (kV)	Peak Counts (Position Relative to sole - inches)	Ideal Position - Calculated (Position Relative to sole - inches)
16(a)	7.5	-4.5	0.032	0.031
16(b)	8.0	-4.0	0.027	0.028
16(c)	8.5	-3.5	0.023	0.026
16(d)	9.25	-2.75	0.019	0.022

The agreement between position of peak counts and the ideal beam position by calculation is quite good. The optimum beam position from the data is 0.005 inches above the plane of the cathode (which is 0.022 inches above the plane of the sole). The trajectories from the cathode to the interaction space can not be calculated by any

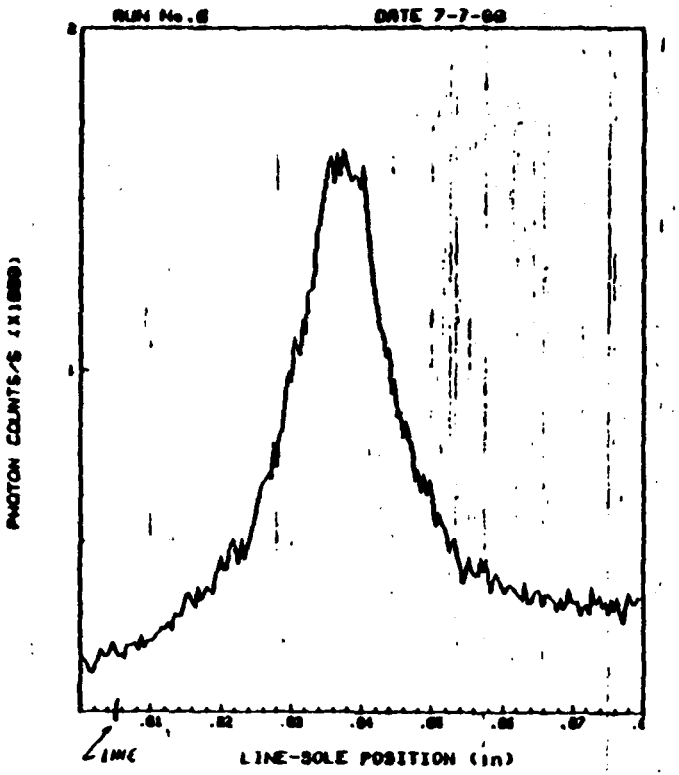

(a) V_k = 7.5 kV, V_s = -4.5 kV, V_a = 4.0 kV

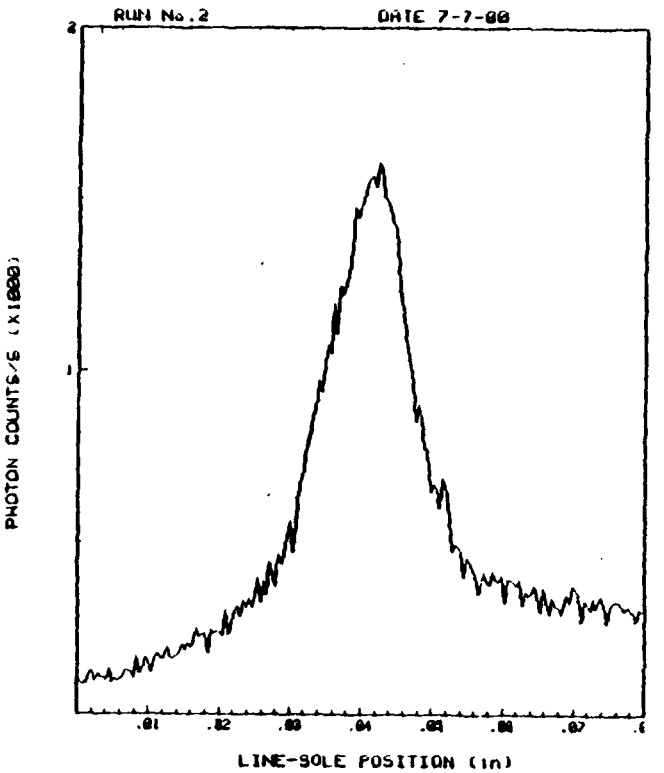

(b) V_k = 8.0 kV, V_s = -4.0 kV, V_a = 3.2 kV

For All Sets of Data: V_g = 0, I_k = 100 mA, B = 3450 Gauss.

Figure 16. Optimization of Beam Injection for Gridded Gun (Continued on Next Page).

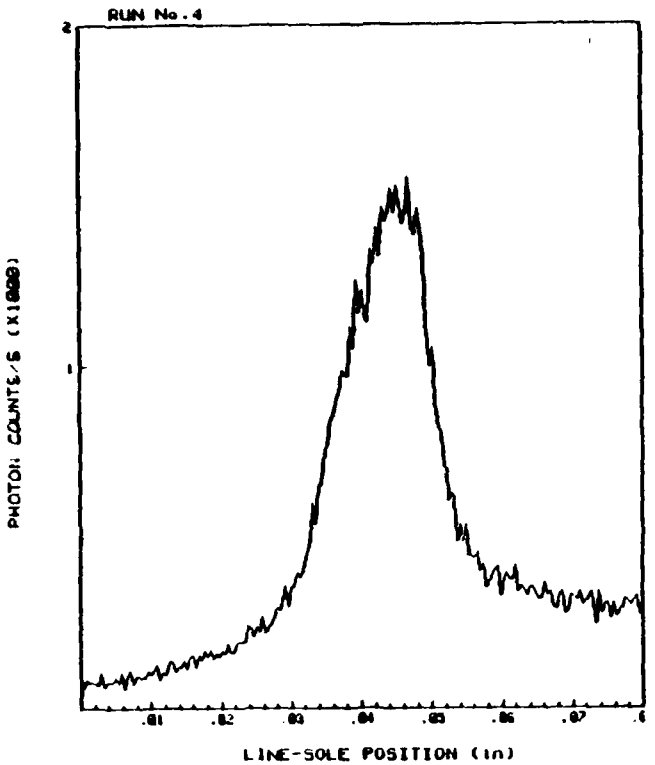

(c) V_k = 8.5 kV, V_s = -3.5 kV, V_a = 3.2 kV

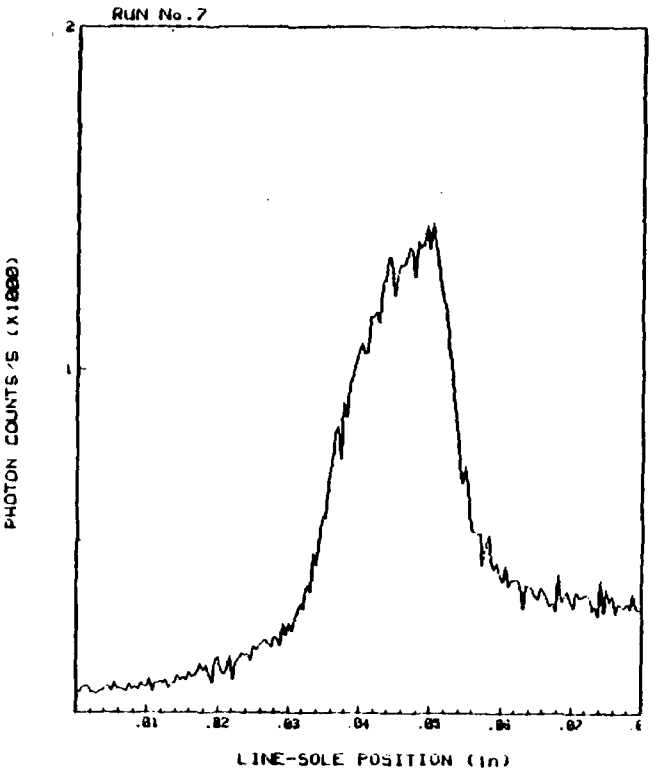

(d) V_k = 9.25 kV, V_s = -2.75 kV, V_a = 2.85 kV

Figure 16. Optimization of Beam Injection for Gridded Gun.

(Continued from Preceding Page)

simple method, first because of the three dimensional configuration of the grid, and second because the fields in the gun region are affected somewhat by the line potential. The latter problem is indicated by the fact that the accelerating anode voltage which is necessary for the same beam current in each case differs for different line voltages.

4.3 UNGRIDDED KINO GUN

Measurements of an ungridded Kino gun are of particular interest because calculations are directly and easily accomplished. The geometry is simple enough that one may reasonably conceive of comparing experimental observations with theoretical analyses of noise. Only the Kino long gun is of great interest. The Kino short gun is, with some exceptions, not capable of supplying enough current for practical applications.

A series of measurements was made to determine the location of a beam injected by the Kino gun. Results are shown in figure 17 for four different combinations of cathode-to-line and cathode-to-sole voltages. In these measurements the line anode, which now incorporates the short section of meander line downstream from the gas jet, is located at 0.005 inches; the sole is located at 0.070 inches. The thinnest beam corresponds to V_k = 8.3 kV and V_s = -2.9 kV. With the Kino gun it is possible to calculate by simple means not only the ideal beam location in the interaction space, but also the trajectories coming out of the gun which should mate ideally with that beam location, assuming ideal electrode shapes. The data from these runs is summarized as follows:

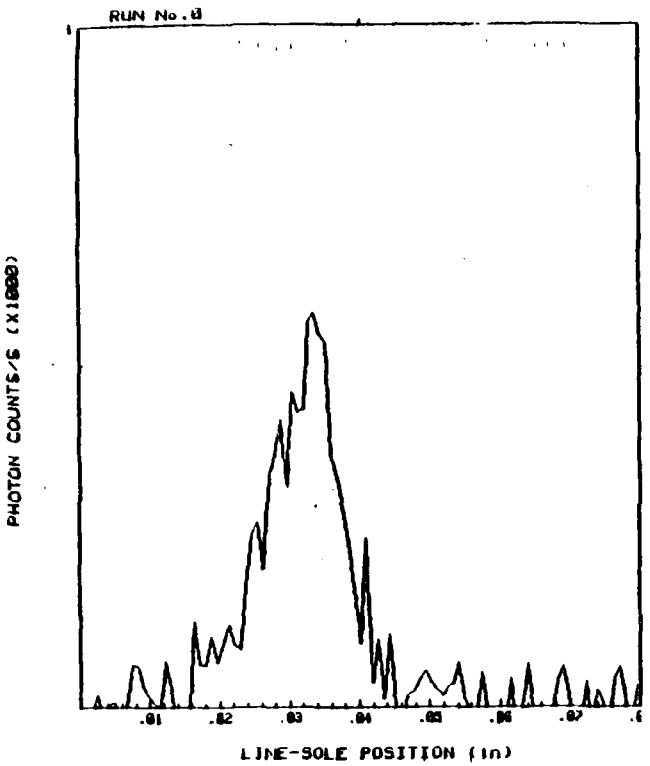

(a) V_k = 8.3 kV, V_s = -2.9 kV

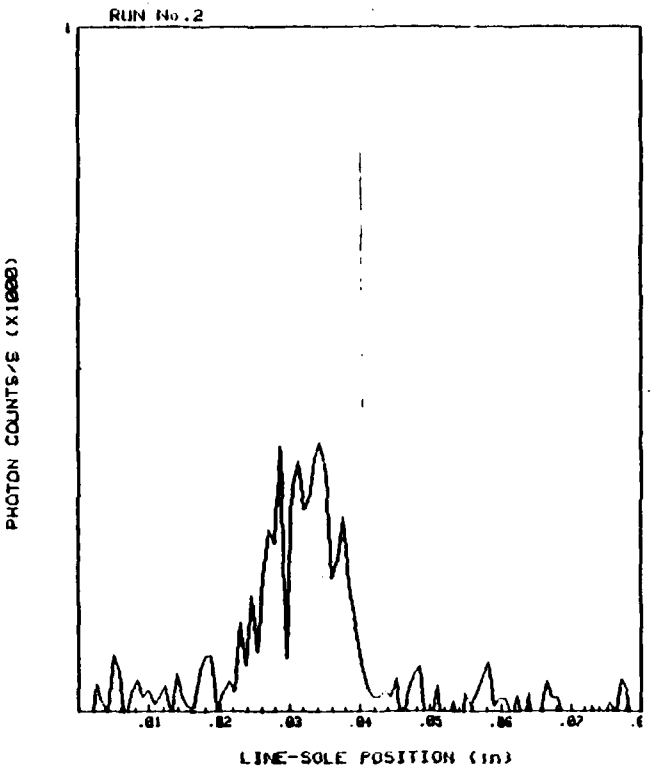

(b) V_k = 8.0 kV, V_s = -3.3 kV

For All Sets of Data:
V_a = 2.2 kV I_k = 1 A
V_g = -25 V B = 2800 Gauss
Cathode Temp. = 1070°C (Brightness)

Figure 17. Beam Position with Kino Gun (Continued on Next Page).

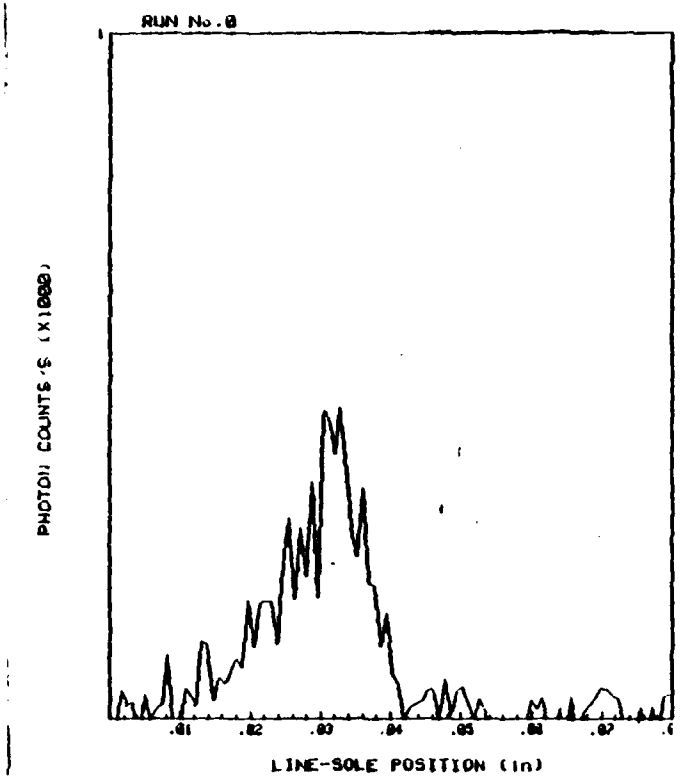

(c) V_k = 7.5 kV, V_S = -4.1 kV

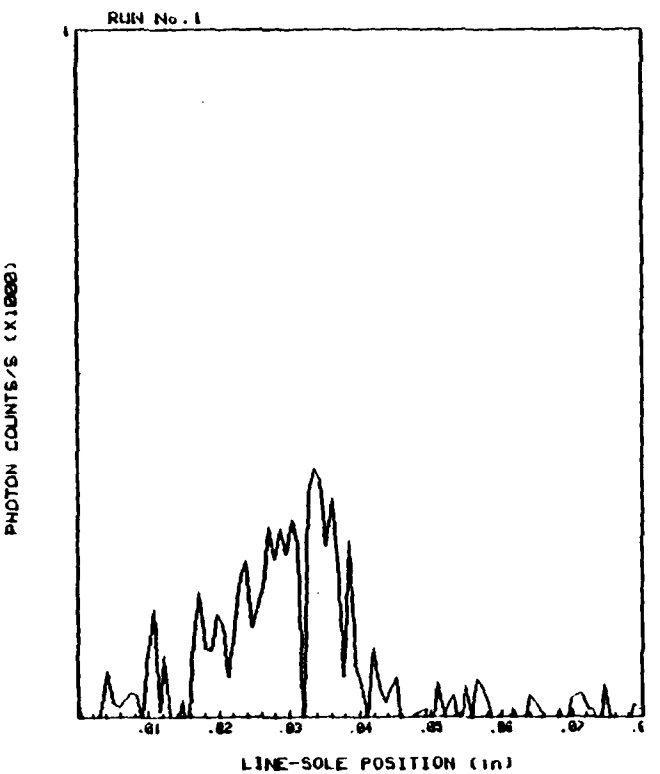

(d) V_k = 7.0 kV, V_S = -4.5kV

Figure 17. Beam Position with Kino Gun (Continued from Previous Page).

Figure	V_k(kV)	V_s(kV)	Peak Counts	Ideal Beam Calculated (Position Relative	Ideal Location of Cathode Surface to Sole - inches)
17(a)	8.3	-2.9	0.036	0.029	0.012
17(b)	8.0	-3.3	0.038	0.031	0.014
17(c)	7.5	-4.1	0.039	0.036	0.017
17(d)	7.0	-4.5	0.038	0.038	0.020

The location of peak counts does not correlate with calculations as well for this set of measurements as for the gridded gun. In these measurements, the peak current was 1.0 A as compared with 0.1 A for the gridded gun. In the present case, space charge was taken into account, while it was not necessary to take space charge into account with 0.1 A beam current. It was assumed, based on the measurements of beam width for the gridded gun (figure 14), that the beam width is 0.155 inches, half the cathode width, and this assumption produces better correlation with measurements than does a beam width of 0.309, the full cathode width. A further discrepancy between calculations and observations is in matching the beam in the interaction space to the beam emerging from the gun. The thinnest beam observed is with V_k = 8.3 kV, for which the ideal location of the cathode plane is 0.011 inch above the sole. The actual cathode location is 0.022 inch above the sole, which most nearly corresponds to V_k = 7.0 kV. But under the latter condition, beam spread is greatest. We must believe that there is some non-ideal condition occurring. Possible explanations are: (1) that there is some serious non-ideal condition in the electrode shapes between the exit plane of the gun and the region in which the electrodes are parallel; (2) that the beam is still narrower than the half width assumed in these calculations.

Figure 18 shows measurements of the same kind made under temperature-limited conditions. Here the beam quality is much poorer than under space-charge limited conditions as in figure 17. Such a result is consistent with the fact that the gun was designed with the space-charge limited assumption.

Beam noise picked up by the meander circuit was observed using a Hewlett-Packard 8555A spectrum analyzer. Results under space-charge limited conditions are shown in figure 19, and for temperature-limited conditions in figure 20. For all sets of conditions, the bandwidth is 300 kHz. For space-charge limited measurements, the reference level (at the top of the screen) is +30 dBm. For temperature-limited measurements, the reference level is +10 dBm.

The most significant observation is the dramatic difference between noise power observed under space-charge limited conditions and under temperature-limited conditions. In the range of highest noise power density observed, about 4 GHz, the temperature-limited observation is less than the space-charge limited observation by more than 30 dB. Another observation is the peaks in the spectrum of the temperature-limited case in the general vicinity of 7 to 7.5 GHz. These appear to be related to the cyclotron frequency in the gun region. It was observed that while the nominal magnetic field is 2800 Gauss, corresponding to 7.84 GHz cyclotron frequency, the effective magnetic field tapers down a little in the direction away from the simulated interaction space. For the very long cathode (0.375 inches) for which the pole pieces of the beam tester were not originally designed, there is a small portion of the cathode in which the magnetic field is as low as 2500 Gauss, for which the cyclotron frequency is 7 GHz. There is no simple theory known to the authors which supports such correlation between noise maxima and cyclotron frequency, but the relationship appears very plausible.

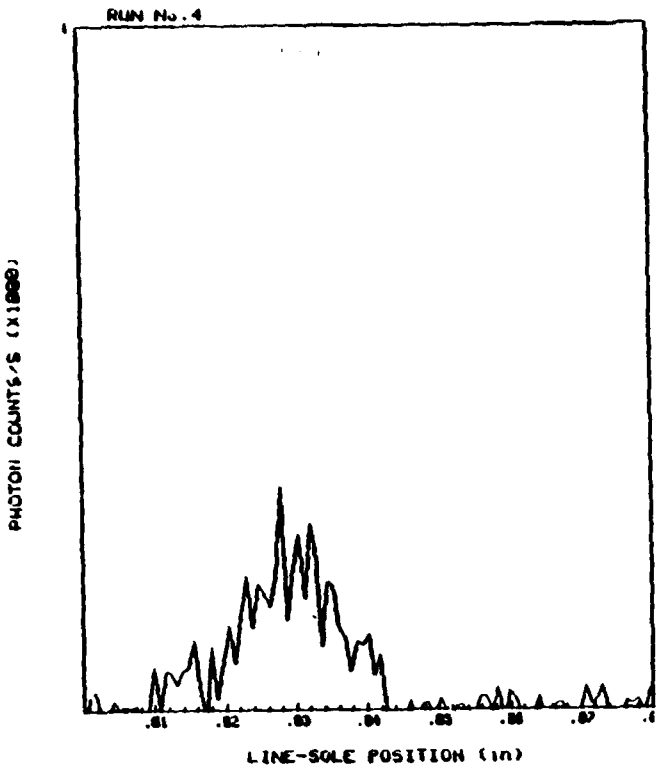

(a) V_k = 7.5 kV, V_s = -4.1 kV

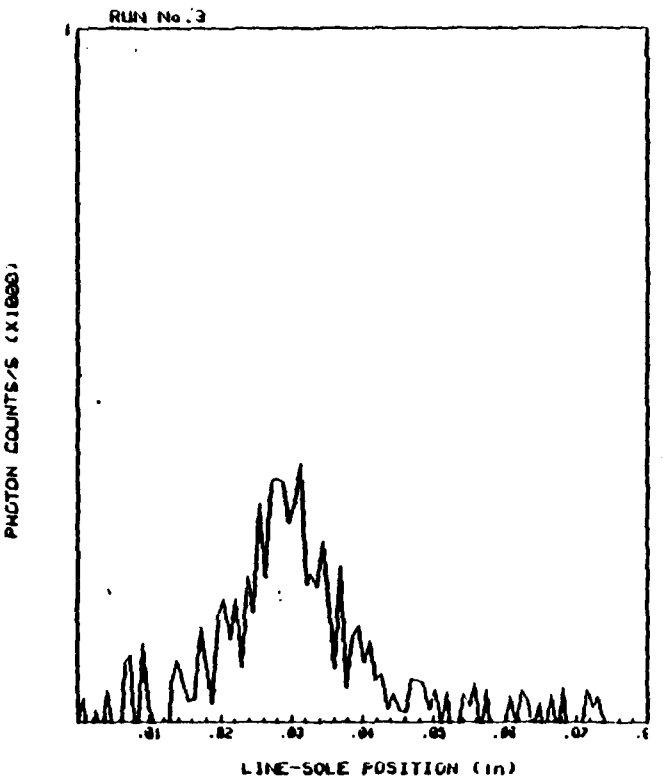

(b) V_k = 8.3 kV, V_s = -2.9 kV

For Both Sets of Data:
V_a = 2.6 kV I_k = 1 A
V_g = -25 V B = 2800 Gauss
Cathode Temperature = 960°C (Brightness)

Figure 18. Beam Position with Temperature - Limited Kino Gun.

A more quantitative analysis of the noise measurements was undertaken, using the resistance factor, R, described in the previous section, to relate noise power observed to noise in the beam. In the computer program to calculate R, a thin laminar beam is assumed and the input data assumed a beam equivalent to the full width of the cathode. Both of these assumptions introduce some small error, but this is not large when with respect to the degree of accuracy with which noise power can be determined from spectrum analyzer observations. For each set of conditions (voltage settings and frequency) a different value of R must be calculated, where power = $1/2i^2R$, and i = peak ac. The value of R also depends upon magnetic field, beam width, and electrode spacings, which were the same for all runs. Cable attenuation was measured and taken into account. A sample set of calculations is shown in Table I for a space-charge limited case and in Table II for a temperature-limited case. The results of all of the calculations are summarized in Table III. The data in figures 19 and 20 were taken when the gas jet was off. Similar photographs were taken when the gas jet was turned on to make the measurements shown in figures 17 and 18. Also included in Table III is the inferred noise at the gun exit when calculated space-charge (diocotron) gain is subtracted from values at the meander circuit. An ideal laminar beam the full width of the cathode again was assumed.

The relationships between beam noise and beam configuration is of interest. The beam which is thinnest and most dense is expected to be noisiest as a result of diocotron gain because the coupling between electrons is greatest. Since conditions are the same in the gun for all four combinations of line and sole voltages, the noise generated in the gun should be about the same for all four cases. The correlation between measurements of noise and beam thickness to the extent it exists shows maximum beam noise for the combination of V_k = 8.0 kV, V_s = 3.3 kV, corresponding to figure 17(b) and 19(b). This is not the most compact beam according to

TABLE I

Calculations for Noise Current: Space-Charge Limited

Operating Conditions: V_k = 7.5 kV, V_s = -4.1 kV, V_a = 2.13 kV, V_g = -25V, I_k = 1.0 A, B = 2800 Gauss

See Figure 19(c) Reference Level: +30 dBm

Frequency (GHz)	Power Readings from Display (dBm) (Note 1)	Power Density (W/GHz)	R Ohms	i^2/GHz (A^2, peak) (Note 2)	Diocotron Gain Calculated (dB)	i^2/GHz at Gun Exit (Note 2)	dB over Shot Noise at Gun Exit (Note 3)
2	-15	0.105	84	0.00251	0.63	0.00217	65
3	- 7	0.665	156	0.00853	1.26	0.00638	70
4	- 7	0.665	222	0.00599	1.89	0.00388	68
5	-11	0.265	268	0.00198	2.52	0.00111	62
6	-12	0.210	286	0.00147	3.15	0.00071	60
7	-13	0.167	274	0.00122	3.78	0.00051	59
8	-16	0.084	238	0.00070	4.41	0.00025	56
9	-18	0.053	187	0.00056	5.04	0.00018	55
10	-19	0.042	134	0.00063	5.67	0.00017	54
11	-25	0.011	91	0.00023	6.30	0.00005	49
12	-32	0.002	61	0.00007	6.93	0.00001	43
13	-35	0.001	39	0.00003	7.56	0.000005	39
				$\sum i^2$ = 0.0239		$\sum i^2$ = 0.0154	
				i_{rms} = 0.11 A		i_{rms} = 0.088 A	

NOTE 1: These are the level on the display taking into account the reference level and the cable losses, in power density/300 kHz. Cable losses vary linearly with frequency from 1 dB at 2 GHz to 3 dB at 12 GHz.

NOTE 2: These are peak currents. Therefore, $i_{rms} = \sqrt{\sum i^2/2}$.

NOTE 3: Shot noise in a 1 A beam is 3.2×10^{-10} A^2 rms.

TABLE II

Calculations for Noise Current: Temperature-Limited

Operating Conditions: V_k = 7.5 kV, V_s = 4.1 kV, V_a = 2.6 kV, V_g = -25V, I_k = 1.0 A, B = 2800 Gauss

Frequency (GHz)	Power Readings from Display (dBm) (Note 1)	Power Density (MW/GHz)	R Ohms	i^2/GHz (A^2, peak) (Note 2)	Diocotron Gain Calculated (dB)	i^2/GHz at Gun Exit (Note 2)	dB over Shot Noise at Gun Exit (Note 3)
2	-50	33	84	0.79×10^{-6}	0.63	0.68×10^{-6}	30
3	-44	133	156	1.7	1.26	1.3	33
4	-40	333	222	3.0	1.89	1.7	34
5	-32	2103	268	15.7	2.52	7.6	41
6	-32	2103	286	14.7	3.15	6.2	40
7	-28	5283	274	38.6	3.78	14.0	43
8	-33	1671	238	14.0	4.41	4.4	38
9	-40	333	187	3.6	5.04	0.97	32
10	-44	133	134	2.0	5.67	0.46	29
11	-47	67	91	1.5	6.30	0.30	27
12	-47	67	61	2.2	6.93	0.38	28
13	-49	42	39	2.1	7.56	0.33	27
14	-50	33	24	2.8	8.19	0.36	28
				$\sum i^2 = 1.026 \times 10^{-4}$		$\sum i^2 = 3.86 \times 10^{-5}$	
				$i_{rms} = 0.0072$ A		$i_{rms} = 0.0044$ A	

For notes, see Table I.

TABLE III

SUMMARY OF NOISE MEASUREMENTS

Figure No.	V_k(kV)	V_s(kV)	Helium Off: i_{rms}(A) at Circuit	Helium Off: i_{rms}(A) at Gun Exit	Helium On: i_{rms}(A) at Circuit
Helium Off					
19(a)	8.3	-2.9	0.14	0.096	0.14
19(b)	8.0	-3.3	0.17	0.116	0.14
19(c)	7.5	-4.1	0.11	0.088	0.15
19(d)	7.0	-4.5	0.11	0.081	0.13
20(a)	7.5*	-4.1	0.007	0.004	0.008

*Temperature-limited

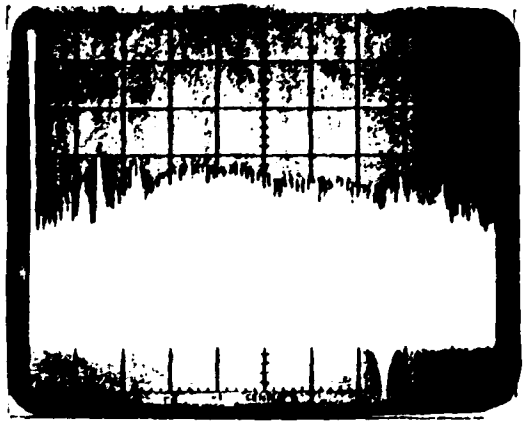

2.07 - 6.15 GHz

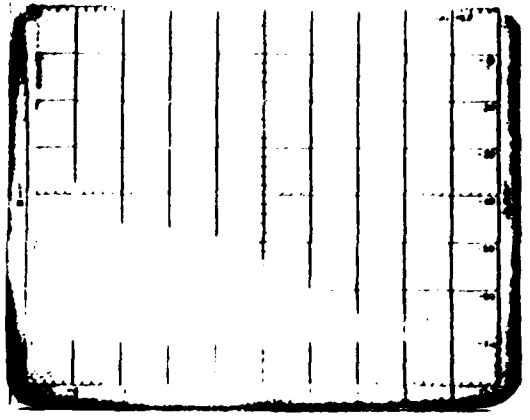

6.23 - 14.35 GHz

(a) V_k = 8.3 kV, V_S = -2.9 kV

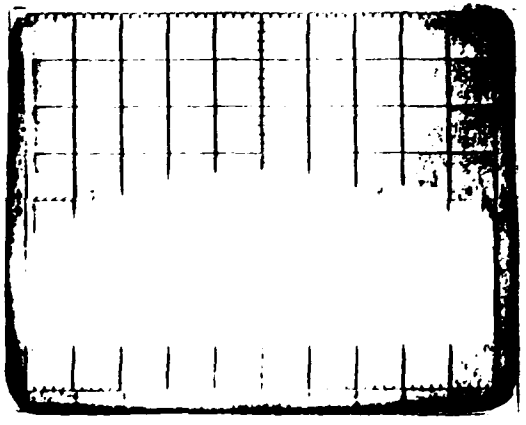

2.07 - 6.15 GHz

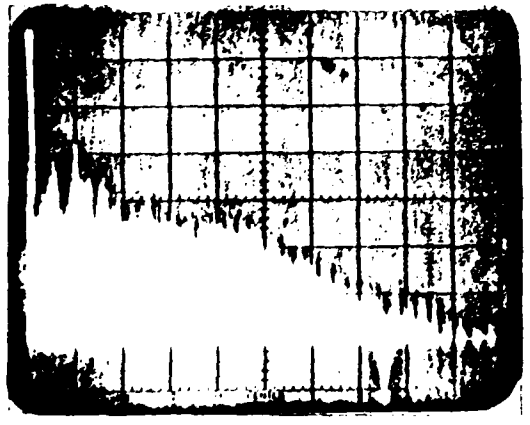

6.23 - 14.35 GHz

(b) V_k = 8.0 kV, V_S = -3.3 kV

Conditions Common to All Spectra: Reference Level = +30 dBm; Other Conditions Like Figure 17.

Figure 19. Output Spectra with Kino Gun (Continued on Next Page)

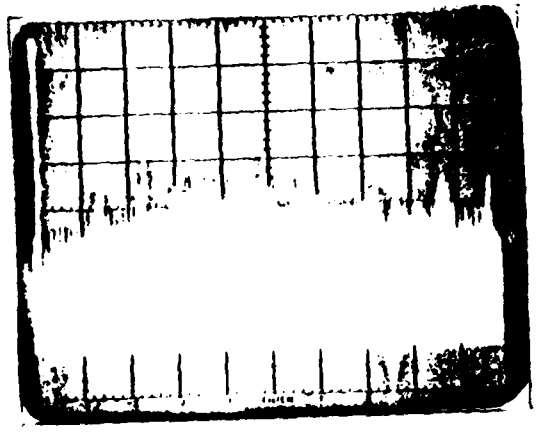

2.07 - 6.15 GHz

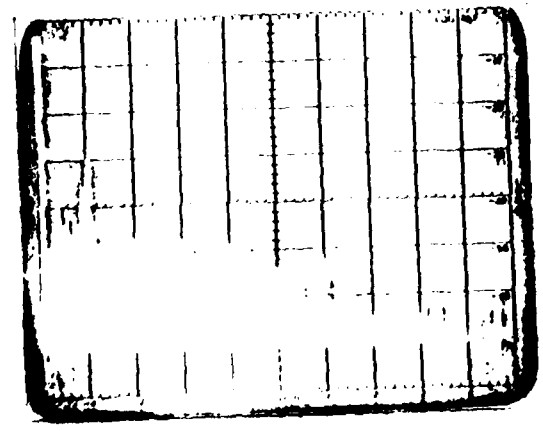

6.23 - 14.35 GHz

(c) V_k = 7.5 kV, V_S =-4.1 kV

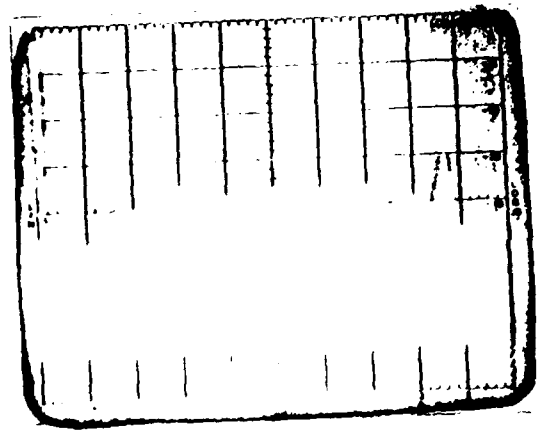

2.07 - 6.16 GHz

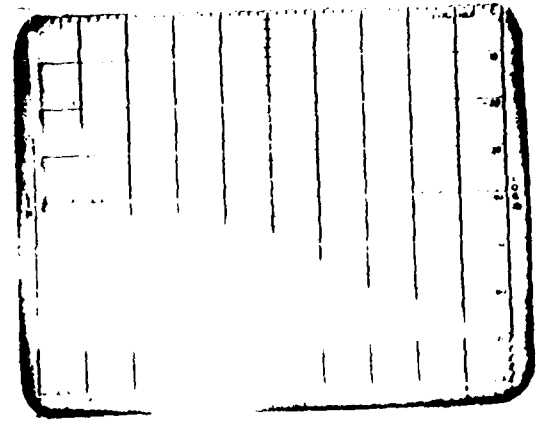

6.23 - 14.35 GHz

(d) V_k - 7.0 kV, V_S =-4.5 kV

Figure 19. Output Spectra with Kino Gun (Continued from Preceding Page)

2.07 - 6.15 GHz

6.23 - 14.35 GHz

Conditions: Reference Level = + 10 dBm
Other Conditions Like Figure 18(c).

Figure 20. Output Spectrum with Temperature - Limited Kino Gun.

figure 17, but it is more compact than those of figures 17(c) and (d), where the noise was less. Note that the noise current at the gun exit is an inferred value assuming an ideal diocotron gain from small signal theory and does not necessarily take into account the actual diocotron gain.

It is also of interest to compare measured beam noise with shot-effect noise. Shot-effect noise current is given by[20]:

$$\overline{i^2} = 2e\, i_o\, f$$

Where $\overline{i^2}$ is the mean square of current fluctuations in a bandwidth f, e is the magnitude of charge on an electron, and I_o is the DC current. Values of shot-effect noise are compared with observed noise in Tables I and II. Note that in Table II, under temperature-limited conditions, the observed noise level is approximately constant at 27 to 30 dB above the shot-noise level except for a range centered around the cyclotron frequency.

SECTION V

SUMMARY AND CONCLUSIONS

The crossed-field beam analyzer has made possible the direct measurement of the configuration of crossed-field beams. In the course of the work reported here, computer control was introduced so that the data taking and print out is automated. A gas beam "chopper" was introduced to suppress spurious responses. As a result, the beam analyzer becomes a much more effective tool in the analysis of crossed-field beams. In addition, a short meander circuit was introduced so that beam noise may be measured directly. Such noise measurements are consistent and reproducible, and give results of sufficient accuracy for most practical purposes. There is no method known to us for verifying the accuracy of these measurements by separate means. The noise figure of an amplifier, for example, incorporates much more uncertainty of measurement than the short meander circuit for noise pick-up which is used here.

Measurement of beam configuration within the gun has been demonstrated for the first time. An inherent deficiency in such measurements is that the gas beam scatters after being injected because it has nowhere else to go. In the simulated interaction space, on the other hand, the gas beam can pass directly through the region being probed. The scattered gas molecules lead to some spurious responses. However, it is still possible to obtain useful data in the gun region if this limitation is taken into account.

It was found that the beam from the gridded gun was substantially narrower than the cathode. Some qualitative observations from autopsies of operating IBCFA's had

indicated that such was the case. The beam narrowing was about the same in the gun as in the simulated interaction space. Non-uniformity of the magnetic field represents a possible cause.

The beam injected from the ungridded Kino gun shows a noise level as much as 70 dB above shot-effect noise, but well below total noise saturation. Arnaud found total noise saturation at the gun exit for a parallel plate gun in a low frequency experiment[6], as mentioned previously in this report. Smol, on the other hand, found quite low noise in beams from Kino guns under some conditions[9].

The most notable observation was the great decrease in beam noise when the cathode became temperature-limited. The difference was more than 30 dB in those parts of the spectrum showing greatest noise under space-charge limited conditions.

It has long been observed that in crossed-fields, beam noise is much less under temperature-limited than space-charge limited conditions. Theoretical studies present various points of view. Some recent theoretical work by several investigators, supported by the Air Force, in fact shows that the potential minimum due to space-charge tends to smooth the noise. The results of these investigations has been summarized by Kooyers and Shaw of UCA Systems, and is reproduced here as Table IV[13]. What is clear is that present theory is still inadequate to give a quantitative explanation of the phenomena observed.

TABLE IV[13]

COMPARISON OF AFOSR CROSSED-FIELD NOISE STUDIES

	Shaw & Kooyers UCA Systems	Fontana MacGregor & Rowe Harris SAI	Harker & Crawford Stanford Univ.	Shkarofsky MPB Technologies
APPROACH	Lagrangian (particle)	Eulerian (fluid) Lagrangian (particle)(1)	Eulerian (fluid)	Eulerian (fluid)
Two-Dimensional Model - Completed	Yes	Yes	Yes	Yes
Three-Dimensional Model - Completed	Yes	-	No	No
Self Consistent Approach	Yes	Yes	No(2)	No(2)
Two-Dimensional Noise Calculations	Yes	No	Yes(3)	Yes(4)
Verified Space Charge Smoothing	Yes	-	Yes	Yes
Verified Diocotron Growth Mechanism	Yes	-	-	-
Capable of Modeling Grids	Yes	Yes	No	No
Detected Feedback to Potential Min. Instab.	No	-	No	No
Capable of Modeling Entire Gun Region	Yes	Yes	No	No
Useful as a Design Tool for CFA Guns	Yes	-	No	No
Three-Dimensional Noise Calculations	Yes	No	No	No

NOTES: (1) Fontana used a fluid approach in the two-dimensional model which gave unsatisfactory results.

(2) Both Harker and Shkarofsky assumed a parabolic d.c. potential at the cathode.

(3) Harker solved for current fluctuations only.

(4) Shkarofsky solved for velocity fluctuations only.

SECTION VI

RECOMMENDATIONS FOR FUTURE WORK

It is recommended that further experimental studies of crossed-field guns be pursued using the apparatus now available. These experiments should include:

1. A range of beam currents.

2. A range of different cathode lengths, requiring construction of additional guns.

3. A more comprehensive study of y-direction effects, i.e., variations parallel to the magnetic field. Are such variations functions of magnetic field or due to other causes?

4. Quantitative measurement of the effects of various means of noise reduction: grid parallel to electron flow, grid perpendicular to electron flow, cathode tilt, etc.

5. Verification of spectrum analyzer quantitative measurements by coupling the output of the meander circuit through a calibrated narrow band filter into a power meter.

In addition, it is appropriate to examine further the mathematical models used in noise investigations. To this end, it is recommended that a systematic exchange in depth of theoretical work, and its relation to experimental results, take place among all recent Air Force contractors studying noise in crossed-fields.

REFERENCES

1. O. Doehler and G. Dohler, "IBCFA Gun Design by Quantitative Beam Analysis", Final Technical Report, AFAL Contract No. F33615-75-1033, May, 1975 to Sept. 30, 1977.

2. D. J. Miley, "IBCFA Gun Engineering Design", Final Technical Report, AFAL Contract No. F33615-78-C-1435, March 15, 1978 to January 15, 1979.

3. G. S. Kino, "A New Type of Crossed Field Electron Gun", Crossed Field Microwave Devices, (E. Okress, ed.) Academic Press Inc., New York, 1961, pp. 164 to 177.

4. T. A. Midford and G. S. Kino, "Some Experiments with a New Type of Crossed-Field Gun", IRE Transactions on Electron Devices, ED-8, p. 324, July 1961.

5. T. A. Midford and G. S. Kino, "Experiments with a New Type Adiabatic Crossed-Field Gun", IRE Transactions on Electron Devices, Vol. ED-9, p. 431, November 1962.

6. J. Arnaud, "Noise in crossed Magnetic and Electric Field Gun", Ann. Radioelect., Vol. 19, pp. 3-20, January 1964.

7. P. Gautier, G. Kantorowicz, J. Nalot, "Le TPOM en impusion", Ann. Radioelect., Vol. 17, January 1962.

8. N. R. Mantena, "Reduction of Noise in Crossed-Field Microwave Amplifiers", Technical Report, ECOM-02164-1, University of California, October 1966.

9. G. Smol, "The Onset of Excess Noise in Crossed-Field Diodes", MOGA Conference, Amsterdam, Netherlands, pp. 8-31, 1970.

10. T. Van Duzer, J. Whinnery, "Noise in Electron Beams", Crossed-Field Microwave Devices (E. Okress, ed.), Vol. 1, pp. 327-357, Academic Press, New York, 1961.

11. F. W. Crawford, "Study of Noise in Crossed-Field Electron Guns", Annual Report No. 1, AFOSR Research No. 77-3306, May 1, 1977 to April 30, 1978, SU-IPR Report No. 745, June, 1978.

12. I. P. Shkarofsky, "Study of Noise in Crossed Field Microwave Devices", Interim Science Report (1977-1978), AFOSR Contract No. F49620-77-C-0106.

13. G. P. Kooyers and E. K. Shaw, "Noise Phenomena in Crossed-Field Electron Beams", Final Technical Report, AFOSR Contract No. F49620-77-C-0061, February 15, 1977 to February 14, 1980.

14. M. L. Sisodia and O. P. Gandhi, "A Study of Noise Behavior of Crossed-Field Electron Guns", MOGA Conference, Cambridge, England, 1966, p. 214.

15. M. L. Sisodia and R. P. Wadhwa, "Noise Reduction in Crossed-Field Guns by Cathode Tilt", Proc. IEEE, Vol. 56, p. 94, January 1968.

16. N. Nichols, Private Communications, RRE, Mavern, England.

17. J. Arnaud and O. Doehler, "Study of Noise in Crossed-Field Guns", JAP, Vol. 33, p. 234, January 1962.

18. F. Diamand, "Etude Experimental du facteur de bruit d'un TPOM en regime continu", 5th International Conference on Microwave Tubes, Paris, p. 169.

19. R. W. Gould, "Space Charge Effects in Beam Type Magnetrons", J. Appl. Phys., Vol. 28, pp. 599-605, 1957.

20. R. G. E. Hutter, Beam and Wave Electronics in Microwave Tubes, p. 356, D. Van Nostrand Co., Princeton, N.J., 1960.